Scheibe, Benjamin; Karttunen, Antti J.; Kraus, Florian

Reactions of ClF_3 with Main Group and Transition Metal Oxides : Access to Dioxychloronium(V) Fluoridometallates and Oxidofluoridometallates

Published in:
European Journal of Inorganic Chemistry

DOI:
10.1002/ejic.202000908

Published: 26/01/2021

Document Version
Publisher's PDF, also known as Version of record

Please cite the original version:
Scheibe, B., Karttunen, A. J., & Kraus, F. (2021). Reactions of ClF_3 with Main Group and Transition Metal Oxides : Access to Dioxychloronium(V) Fluoridometallates and Oxidofluoridometallates. *European Journal of Inorganic Chemistry*, *2021*(4), 405-421. https://doi.org/10.1002/ejic.202000908

EurJIC
European Journal of Inorganic Chemistry

Full Papers
doi.org/10.1002/ejic.202000908

Chemistry
Europe
European Chemical
Societies Publishing

Reactions of ClF$_3$ with Main Group and Transition Metal Oxides: Access to Dioxychloronium(V) Fluoridometallates and Oxidofluoridometallates

Benjamin Scheibe,[a] Antti J. Karttunen,[b] and Florian Kraus*[a]

Compounds containing the dioxychloronium cation, [ClO$_2$]$^+$, were obtained from reactions of ClF$_3$ with various oxides such as TiO$_2$, MoO$_3$, Re$_2$O$_7$, SnO, P$_2$O$_5$, As$_2$O$_5$, and Nb metal, as the latter contained oxide as an impurity. Partial hydrolysis of [ClF$_2$][IrF$_6$] led to the formation of [ClO$_2$][IrF$_6$]. The crystal structures of the compounds were determined by single-crystal X-ray diffraction, which showed that depending on the starting material [ClO$_2$]$^+$ salts with the fluoridometallate anions [TiF$_{3/2}$F$_{3/1}$]$_2$]$^-$, [Nb$_3$F$_{16}$]$^-$, [IrF$_6$]$^-$, [SnF$_{2/2}$F$_{4/1}$]$^-$ [PF$_6$]$^-$, and [AsF$_6$]$^-$, or with the oxidofluoridometallate anions [Mo$_3$O$_3$F$_{13}$]$^-$ and [Re$_3$O$_6$F$_{10}$]$^-$, were obtained. Bent [ClO$_2$]$^+$ cations with short Cl$\cdots\mu$–F contacts of surrounding F atoms of the anions with the Cl atom are present in the crystal structures, leading to coordination numbers of 2+4 or 2+6 for the Cl atom. Various structural motifs are observed, which range from molecular, columnar, ladder-like, to layer and framework structures. The salts were furthermore characterized by Raman spectroscopy and solid-state quantum-chemical calculations. Covalent Cl–O bonds and ionic Cl$\cdots\mu$–F interactions are indicated by the calculations.

Introduction

Chlorosyl fluoride, ClOF, has a short lifetime and disproportionates into ClF and ClO$_2$F.[1–4] The latter, called chlorine dioxide fluoride or chloryl fluoride, is one of the known stable oxyfluorides of chlorine.[5–8] The other ones are chlorine oxide trifluoride ClOF$_3$, perchloryl fluoride ClO$_3$F, and chlorine dioxide trifluoride ClO$_2$F$_3$.[9–14] Perchloryl hypofluorite, ClO$_4$F, does not possess a Cl–F bond, as indicated by the name, and is thus different from the oxyfluorides.[8,15] Structural formulas of these compounds are shown in Scheme 1.

ClO$_2$F can be synthesized by different methods, the most important ones being the fluorination of ClO$_2$ (Equation (1)) or of chlorates, *A*[ClO$_3$] (*A*=Na, K) (Equation (2) and Equation (3)).[5,8,16–19]

$$2\ \mathrm{ClO_2} + \mathrm{F_2} \rightarrow 2\ \mathrm{ClO_2F} \tag{1}$$

$$6\ \mathrm{K[ClO_3]} + 10\ \mathrm{BrF_3} \rightarrow 6\ \mathrm{K[BrF_4]} + 2\ \mathrm{Br_2} + 3\ \mathrm{O_2} + 6\ \mathrm{ClO_2F} \tag{2}$$

$$\begin{gathered} 6A[\mathrm{ClO_3}] + 4\ \mathrm{ClF_3} \rightarrow 6\ A\mathrm{F} + 2\ \mathrm{Cl_2} + 3\ \mathrm{O_2} + 6\ \mathrm{ClO_2F} \\ A = \mathrm{Na, K} \end{gathered} \tag{3}$$

Reactions involving the chlorine oxides ClO$_2$ or Cl$_2$O$_6$ are usually disadvantageous due to their preparation and handling.[5,16,20,21] Usage of BrF$_3$ usually leads to Br$_2$ impurities in the ClO$_2$F, in comparison to the fluorination with ClF$_3$, which gives more easily separable Cl$_2$ as a side product. If the chlorates are fluorinated with gaseous F$_2$, both ClO$_2$F and ClO$_3$F are formed.[6,22,23] ClO$_2$F is furthermore formed in the reactions of ClF, ClF$_3$, and ClF$_5$ with many oxygen-containing compounds.[8,24,25]

ClO$_2$F can act as an oxidizing and fluorinating agent, but it is much less oxidizing than ClF$_3$.[8] Like other halogen fluorides and oxyfluorides, it shows amphoteric behavior and thus can act as a Lewis acid or base. The halogen dioxide fluorides, *X*O$_2$F (*X*=Cl, Br, I), form bent C_{2v} [*X*O$_2$]$^+$ cations with Lewis acids such as AsF$_5$ or SbF$_5$ (Equation (4)).[19,26–33]

$$\begin{gathered} X\mathrm{O_2F} + M\mathrm{F_5} \rightarrow [X\mathrm{O_2}][M\mathrm{F_6}] \\ X = \mathrm{Cl, Br, I};\ M = \mathrm{As, Sb} \end{gathered} \tag{4}$$

Compounds with [ClO$_2$]$^+$ or [BrO$_2$]$^+$ ions are furthermore obtained when *X*O$_3$F (*X*=Cl, Br) is reacted with strong Lewis acids.[34] In the case of [ClO$_2$]$^+$ cations, reactions of Cl$_2$O$_6$ ("[ClO$_2$][ClO$_4$]") with metals or chlorides often lead to the formation of dioxychloronium(V) perchloratometallates, where [ClO$_4$]$^-$ anions are bound as ligands.[35–40] Crystal structures of [ClO$_2$]$^+$ salts with the following anions have been reported: [BF$_4$]$^-$, [GeF$_{2/2}$F$_{4/1}$]$^-$, [RuF$_6$]$^-$, [SbF$_6$]$^-$, [Sb$_2$F$_{11}$]$^-$, [ClO$_4$]$^-$, [Au(ClO$_4$)$_4$]$^-$ and [Sn(ClO$_4$)$_6$]$^{2-}$.[34,37–44] Recently, compounds were published containing the complex [Cl$_2$BrO$_6$]$^+$ cation that might be considered as a central [BrO$_2$]$^-$ anion coordinating to two [ClO$_2$]$^+$ cations.[45]

Salts containing disphenoidal (seesaw) C_{2v} [*X*O$_2$F$_2$]$^-$ anions are also known but they are usually not formed by the direct reaction of *X*O$_2$F with a fluoride ion donor.[46–49] Thus far, only salts with [IO$_2$F$_2$]$^-$ anions have been structurally characterized by single-crystal X-ray diffraction.[49–52] For Cl, the direct reaction

---

[a] B. Scheibe, Prof. Dr. F. Kraus
Fachbereich Chemie, Philipps-Universität Marburg
Hans-Meerwein-Straße 4, 35032 Marburg, Germany
E-mail: f.kraus@uni-marburg.de
[b] Prof. Dr. A. J. Karttunen
Department of Chemistry and Materials Science
Aalto University
00076 Aalto, Finland

Supporting information for this article is available on the WWW under https://doi.org/10.1002/ejic.202000908

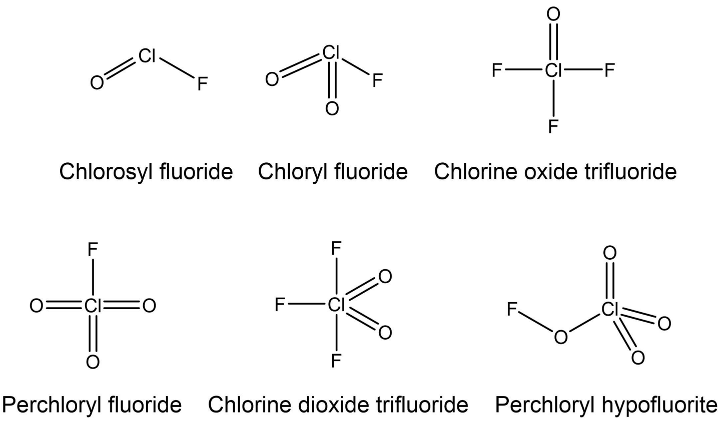

Scheme 1. Overview of the known hypofluorite and oxyfluorides of chlorine.

of ClO_2F with CsF, yielding $Cs[ClO_2F_2]$, is known, and for Br, the reaction of BrO_2F with KF, giving $K[BrO_2F_2]$, accompanied with the partial decomposition of BrO_2F during this reaction, has been reported.[47,48,53] The indirect formation via hydrolysis reactions of $K[BrF_6]$ or fluorination of $K[BrO_3]$ with BrF_5 is also possible, but $K[BrOF_4]$ is usually also formed.[29–31,48] The corresponding iodine compounds can be synthesized by dissolving an iodate, $A[IO_3]$ (A = Na, K, Rb, Cs, NH_4, $N(CH_3)_4$), in hydrofluoric acid.[50,54]

Here, we report on reactions of ClF_3 with the main group oxides SnO, P_2O_5, and As_2O_5, and with the transition metal oxides TiO_2, Nb/Nb_2O_5, MoO_3, and Re_2O_7, as well as on the hydrolysis reaction of $[ClF_2][IrF_6]$. These reactions lead to the formation of dioxychloronium(V) salts with the fluoridometallate anions $[Ti_2F_9]^-$, $[SnF_5]^-$, $[MF_6]^-$ (M = Ir, P, As), and $[Nb_3F_{16}]^-$ and to the oxidofluoridometallate anions $[Mo_3O_3F_{13}]^-$ and $[Re_3O_6F_{10}]^-$. Crystal structures were determined by single-crystal X-ray diffraction and the compounds were further characterized by Raman spectroscopy and quantum-chemical calculations.

Results and Discussion

Syntheses of $[ClO_2]^+$ compounds

Compounds containing the $[ClO_2]^+$ cation are usually synthesized by the reaction of ClO_2F with a Lewis acid.[7,8,26,55] It is known that ClF_3, when reacted with oxygen-containing compounds such as H_2O, forms ClO_2F along other side-products.[1,8,24,25] This might be attributed to the intermediate formation of ClOF, an elusive oxyfluoride that readily disproportionates into ClO_2F and ClF.[1–4] Furthermore, $[ClO_2]^+$ impurities were reported in reactions of ClF_3 with Lewis acids, where either ClF_3 was contaminated with ClO_2F, or when the starting material contained water or the equipment was not properly dried or "unsuitable" for the work with ClF_3, for example, apparatuses made out of glass.[8,55,56] The reactions of ClF_3 with main group (non)metal and transition metal oxides of elements that can form fluoridometallate or oxidofluoridometallate anions were studied (Equations (5) to (10)).

Caution! We would like to stress that the reactions of ClF_3 with metal powders or oxides are highly exothermic and can result in explosions when scaled up.

In all cases, salts containing the $[ClO_2]^+$ cation were obtained, as shown by single-crystal X-ray diffraction and Raman spectroscopy. Furthermore, the hydrolysis reaction of $[ClF_2][IrF_6]$ yielded $[ClO_2][IrF_6]$ and the reaction of Nb powder that had been stored on air, gave $[ClO_2][Nb_3F_{16}]$ along with $[ClF_2][NbF_6]$.[57] All given equations are idealized and assume that ClO_2F and/or ClF are the sole side-products in these reactions. ClO_2F and ClF are themselves oxidizing and fluorinating agents, and depending on the reaction conditions, O_2 and Cl_2 might also be formed.[8]

The reactions of M_2O_5 (M = P, As) with ClF_3 lead to the formation of $[ClO_2][MF_6]$ (Equation (5)). While the reaction of P_2O_5 with ClF_3 is highly exothermic and vigorous, the reaction with As_2O_5 is comparably slow. The dissociation pressure of the adduct $[ClO_2][PF_6]$ is high and it is unstable at room temperature.[26]

$$\begin{gathered}2\,M_2O_5 + 10\,ClF_3 \rightarrow 4\,[ClO_2][MF_6] + ClO_2F + 5\,ClF \\ M = \mathrm{P, As}\end{gathered} \tag{5}$$

The reaction of SnO with ClF_3 in anhydrous HF (aHF) leads to the formation of $[ClO_2][SnF_5]$ and likely $[ClF_2][SnF_5]$ as well, as bands of the $[ClF_2]^+$ cation show up in the Raman spectrum (Equation (6)).

$$2\,SnO + 5\,ClF_3 \xrightarrow{aHF} [ClO_2][SnF_5] + [ClF_2][SnF_5] + 3\,ClF \tag{6}$$

If TiO_2 is reacted with ClF_3, then $[ClO_2][Ti_2F_9]$ is formed (Equation (7)).

$$2\,TiO_2 + 4\,ClF_3 \rightarrow [ClO_2][Ti_2F_9] + ClO_2F + 2\,ClF \tag{7}$$

The reaction of MoO_3 with ClF_3 yields a salt containing the $[Mo_3O_3F_{13}]^-$ anion (Equation (8)). The reaction of $MoOF_4$ with ClF_3 also gave the compound $[ClO_2][Mo_3O_3F_{13}]$, assuming the formation of MoF_6 (Equation (9)).

$$3\ MoO_3 + 6\ ClF_3 \rightarrow [ClO_2][Mo_3O_3F_{13}] + 2\ ClO_2F + 3\ ClF \tag{8}$$

$$5\ MoOF_4 + 2\ ClF_3 \rightarrow [ClO_2][Mo_3O_3F_{13}] + 2\ MoF_6 + ClF \tag{9}$$

Carried out at −37 °C, the reaction of Re_2O_7 with ClF_3 leads to a salt with the $[Re_3O_6F_{10}]^-$ anion (Equation (10)). Crystals of the compound quickly decompose at room temperature. The reactions of Re_2O_7 with ClF_3 were reported previously and depending on the reaction conditions, ReO_2F_3 (at low temperatures) or $ReOF_5$ (room temperature) was formed.[58,59]

$$6\ Re_2O_7 + 18\ ClF_3 \rightarrow 4\ [ClO_2][Re_3O_6F_{10}] + 5\ ClO_2F + 9\ ClF \tag{10}$$

During the attempted synthesis of a salt with a $[ClF_2(ClF_3)_n]^+$ cation that would be similar to the cations $[BrF_2(BrF_3)_n]^+$ ($n=1$, 2), the salt $[ClO_2][IrF_6]$ was obtained as a hydrolysis product (Equation (11)).[60] Hydrolysis reactions of $[ClF_2]^+$ salts, yielding $[ClO_2]^+$ salts, were previously reported.[25,61]

$$ClF_2[IrF_6] + 2\ H_2O + ClF_3 \rightarrow [ClO_2][IrF_6] + 4\ HF + ClF \tag{11}$$

Crystal structures of $[ClO_2]^+$ compounds

The crystal structure of $[ClO_2][PF_6]$

Dioxychloronium(V) hexafluoridophosphate(V) crystallizes in the orthorhombic space group $P2_12_12_1$ (No. 19) with four formula units per unit cell, Pearson code *oP*40, and Wyckoff sequence 19.a^{10}. Selected crystallographic data and details of the structure determination are given in Table 1. Atomic coordinates, equivalent isotropic and anisotropic displacement parameters are reported in the Supporting Information. The Cl(1) atom occupies the Wyckoff position 4*a* (site symmetry 1) and is surrounded by the two oxygen atoms O(1) and O(2), giving the $[ClO_2]^+$ cation (Figure 1). The Cl–O bond lengths are 1.4077(8) and 1.4060(8) Å and the O–Cl–O angle is 119.75(5)°. A comparison of the Cl–O bond lengths of the investigated compounds and thus far reported $[ClO_2]^+$ salts is given in Table 2.

The P(1) atom also occupies a general position (4*a*) and is surrounded by the six fluorine atoms F(1) to F(6) in the shape of a distorted octahedron, yielding the $[PF_6]^-$ anion. The P−F bond lengths lie in the range from 1.5881(6) to 1.6197(6) Å and nicely agree with those in Li[PF_6], which are 1.603(1) Å at room temperature.[62] Five of the six F atoms, F(1) and F(3) to F(6), show short Cl⋯μ–F contacts with the Cl atom with distances in the range of 2.6226(7) to 2.8797(7) Å. The F(4) atom shows

Table 1. Selected crystallographic data and details of the structure determinations of $[ClO_2][MF_6]$ ($M=$ P, As, Ir), $[ClO_2][SnF_5]$, $[ClO_2][Ti_2F_9]$ and $[ClO_2][Nb_3F_{16}]$.

Compound	$[ClO_2][PF_6]$	$[ClO_2][AsF_6]$	$[ClO_2][IrF_6]$	$[ClO_2][SnF_5]$	$[ClO_2][Ti_2F_9]$	$[ClO_2][Nb_3F_{16}]$
Molar mass [$g \cdot mol^{-1}$]	212.42	256.37	373.65	281.14	334.25	650.18
Space group (No.)	$P2_12_12_1$(19)	$C2/m$(12)	$P12/n1$(13)	$P12_1/n1$(14)	$C2/c$(15)	$C2/c$(15)
a [Å]	5.2060(3)	10.9411(6)	7.0660(4)	7.3673(4)	11.084(2)	9.6738(7)
b [Å]	10.1459(5)	10.0225(5)	5.6559(3)	5.1042(3)	14.603(2)	14.4023(11)
c [Å]	10.2172(5)	5.0773(3)	7.1583(4)	13.5108(8)	5.330(1)	10.0266(8)
β [°]	90	97.680(5)	92.052(1)	93.026(2)	111.73(1)	97.142(3)
V [$Å^3$]	539.67(5)	551.77(5)	285.90(3)	507.35(5)	801.4(2)	1386.1(2)
Z	4	4	2	4	4	4
Pearson symbol	*oP*40	*mS*40	*mP*20	*mP*36	*mS*56	*mS*88
$\rho_{calc.}$ [$g \cdot cm^{-3}$]	2.61	3.09	4.34	3.68	2.77	3.12
μ [mm^{-1}]	1.084	6.722	23.891	5.606	2.459	2.816
Color	colorless	colorless	yellow	colorless	colorless	colorless
Crystal morphology	block	block	block	block	block	block
Crystal size [mm^3]	0.39×0.46×0.49	0.10×0.15×0.26	0.15×0.24×0.27	0.05×0.06×0.12	0.09×0.13×0.25	0.18×0.18×0.23
T [K]	100					
λ [Å]	0.71073 (Mo-K_α)					
No. of reflections	18116	6480	43352	9560	14689	47929
θ range [°]	2.83–41.25	3.76–33.33	3.60–41.39	3.02–33.19	2.79–31.50	2.55–39.59
Range of Miller indices	$-9 \leq h \leq 8$ $-18 \leq k \leq 18$ $-18 \leq l \leq 18$	$-16 \leq h \leq 16$ $-15 \leq k \leq 15$ $-7 \leq l \leq 7$	$-13 \leq h \leq 13$ $-10 \leq k \leq 10$ $-13 \leq l \leq 13$	$-11 \leq h \leq 11$ $-7 \leq k \leq 7$ $-20 \leq l \leq 20$	$-16 \leq h \leq 14$ $-21 \leq k \leq 21$ $-7 \leq l \leq 7$	$-17 \leq h \leq 17$ $-25 \leq k \leq 25$ $-17 \leq l \leq 17$
Absorption correction	multi-scan	integration	multi-scan	multi-scan	integration	multi-scan
$Trans._{max}$, $Trans._{min}$	0.28, 0.22	0.56, 0.29	0.11, 0.01	0.75, 0.62	0.84, 0.58	0.44, 0.38
R_{int}, R_σ	0.0249, 0.0337	0.0186, 0.0373	0.0159, 0.0269	0.0315, 0.0355	0.0421, 0.475	0.0126, 0.291
Completeness of the data set	0.999	0.998	0.997	0.997	0.999	0.996
No. of unique reflections	3598	1126	1927	1934	1337	4167
No. of parameters	92	51	47	83	66	102
No. of restraints	0	0	0	0	0	0
No. of constraints	0	0	0	0	0	0
S (all data)	1.089	1.113	1.146	1.034	1.017	1.191
$R(F)$ ($I \geq 2\sigma(I)$, all data)	0.0203, 0.0240	0.0184, 0.0253	0.0216, 0.0225	0.0222, 0.0344	0.0452, 0.0616	0.0137, 0.0155
$wR(F^2)$ ($I \geq 2\sigma(I)$, all data)	0.0432, 0.0443	0.0410, 0.0435	0.0614, 0.0623	0.0403, 0.0434	0.1101, 0.1218	0.0310, 0.0315
Flack parameter x	0.00(2)	–	–	–	–	–
Extinction coefficient	0.064(3)	not refined	not refined	0.0040(3)	0.0097(18)	0.00189(8)
$\Delta\rho_{max}$, $\Delta\rho_{min}$ [$e \cdot Å^{-3}$]	0.38, −0.35	0.41, −0.65	4.30, −4.45	0.82, −0.90	0.82, −0.94	0.95, −0.65

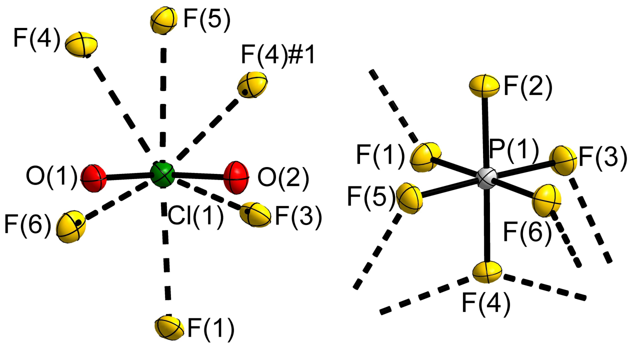

Figure 1. The coordination environment of the Cl and P atom in the crystal structure of $[ClO_2][PF_6]$. Short contacts of F atoms belonging to the $[PF_6]^-$ anions with neighboring Cl atoms are shown as dashed bonds. Symmetry transformation: #1 1/2$-x$, 1$-y$, 1/2$+z$. Displacement ellipsoids are shown at the 70% probability level at 100 K.

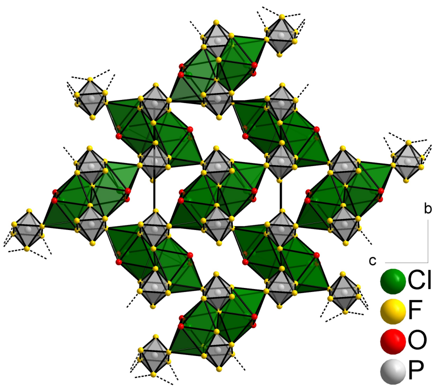

Figure 2. Crystal structure of $[ClO_2][PF_6]$ projected along the *a* axis. Coordination polyhedra of Cl atoms are shown in green and those of P atoms in grey. Short contacts of F atoms belonging to the $[PF_6]^-$ anions with neighboring Cl atoms are shown as dashed bonds. Atoms are shown as isotropic with arbitrary radii.

contacts to two Cl atoms and is μ_3-bridging. With the P–μ_3–F bond being the longest, the P–μ–F bonds are significantly longer compared to the terminally bound F(2) atom with a P–F bond length of 1.5881(6) Å. They range from 1.5993(7) to 1.6197(6) Å. This is likely due to the higher effective coordination number of these μ–F atoms and their interaction with the Cl atom.

The overall coordination number of the Cl atom is 2+6 if the μ–F atoms are considered and the F and O ligands are arranged in the shape of a distorted square antiprism (Figure 1). Due to the shorter Cl–O bonds in comparison to the much longer Cl$\cdots\mu$–F interactions, the Cl atom is displaced from the center of the coordination polyhedron. In comparison to previously reported crystal structures of $[ClO_2]^+$ compounds, such as $[ClO_2][BF_4]$, $[ClO_2][RuF_6]$, $[ClO_2][SbF_6]$, $[ClO_2][Sb_2F_{11}]$, or $[ClO_2][ClO_4]$, the coordination number of the Cl atom is unexpectedly high.[34,39,41,43,44] Usually, only four short contacts of O or F atoms from surrounding anions are observed. The only other example with such a coordination number for the Cl atom of a $[ClO_2]^+$ cation is the compound $[ClO_2][GeF_5]$, in which two symmetry-independent $[ClO_2]^+$ cations are present. There, one Cl atom has coordination number six (distorted octahedron) and the other one eight (square antiprism).[41]

When these Cl$\cdots\mu$–F contacts are considered, a framework structure is obtained (Figure 2). The structure can be described with the Niggli formula$_\infty{}^3\left[\langle ClF_{\frac{2}{2+1}}F_{\frac{4}{1+1}}O_{\frac{2}{1}}\rangle\langle PF_{\frac{1}{1+2}}F_{\frac{4}{1+1}}F_{\frac{1}{1}}\rangle\right]$, where the notation of the Niggli formula is given according to the literature.[63] Explained in short, this type of Niggli formula indicates for the cation that two F atoms bridge μ_3-like between two Cl and one P atoms, four F atoms bridge between the Cl and P atoms, and the two O atoms belong solely to the Cl atom. For the anion, there is one μ_3-like bridging F atom between one P and two Cl atoms, there are four μ-like bridging F atoms between a P and a Cl atom, and there is one terminally bound F atom.

The Cl atoms form a hexagonal close packing, with Cl$\cdots$Cl distances of *circa* 5.21 to 6.64 Å. When Cl$\cdots$P distances of 3.64 to 5.11 Å are considered, a distorted octahedron for the P atom and a distorted trigonal prism for the Cl atom are obtained as the coordination polyhedra. The arrangement of the P and Cl atoms is therefore similar to the Ni and As atoms in the NiAs structure type.[64]

The crystal structure of $[ClO_2][AsF_6]$

To our surprise, dioxychloronium(V) hexafluoridoarsenate(V) is not isotypic to the $[PF_6]^-$ salt described above and crystallizes

Table 2. Experimental and calculated Cl–O bond lengths, as well as Cl$\cdots\mu$–F distances of bridging F atoms of fluoridometallate and oxidofluoridometallate anions in $[ClO_2]^+$ salts.

Compound	Bond lengths and atomic distances [Å]		Calculated bond lengths and atomic distances (DFT-PBE0/TZVP, solid-state) [Å]	
	Cl–O	Cl$\cdots\mu$–F	Cl–O	Cl$\cdots\mu$–F
$[ClO_2][PF_6]$	1.4060(8), 1.4077(8)	2.6226(7)–2.8797(7)	1.43, 1.44	2.50–2.82
$[ClO_2][AsF_6]$	1.4027(11)	2.7275(9), 2.7953(8)	1.44	2.58, 2.77
$[ClO_2][IrF_6]$	1.409(3)	2.467(2), 2.699(2)	1.44	2.32, 2.77
$[ClO_2]SnF_5$	1.4045(13), 1.4050(18)	2.3847(14)–2.6912(14)	1.44	2.30–2.68
$[ClO_2]Ti_2F_9$	1.401(3)	2.665(2), 2.708(2)	1.44	2.56, 2.66
$[ClO_2][Nb_3F_{16}]$	1.4084(6)	2.4904(5), 2.6554(6)	1.44	2.39, 2.63
$[ClO_2][Mo_3O_3F_{13}]$	1.3950(18), 1.4068(18)	2.4617(15)–2.9054(15)	1.43	2.39–2.85
$[ClO_2][Re_3O_6F_{10}]$	1.384(4), 1.418(4)	2.354(3)–2.749(3)	1.44	2.25–2.82

with four formula units per unit cell in the monoclinic space group *C*2/*m* (No. 12), Pearson code *mS*40, and Wyckoff sequence 12.j^3i^3h. Selected crystallographic data and details of the structure determination are given in Table 1. Atomic coordinates, equivalent isotropic and anisotropic displacement parameters are reported in the Supporting Information. The Cl(1) atom occupies the Wyckoff position 4 *h* (site symmetry 2) and is surrounded by the oxygen atoms O(1) and O(1)#1, giving the $[ClO_2]^+$ cation (Figure 3). The Cl–O bond length is 1.4027(11) Å and the O–Cl–O angle is 119.57(11)°. The As(1) atom occupies the Wyckoff position 4*i* (site symmetry *m*) and is surrounded by six F atoms in the shape of a distorted octahedron, resulting in the $[AsF_6]^-$ anion. The As–F bond lengths lie in the range of 1.7034(14) to 1.7418(13) Å and are comparable to those in Li[AsF_6], which are 1.74(4) Å at room temperature.[62] The F atoms of the $[AsF_6]^-$ anion show short Cl···μ–F contacts of either 2.7275(9) or 2.7953(8) Å. One of the F atoms of the $[AsF_6]^-$ anion, F(4), is μ_3-bridging, two are μ-bridging, F(2) and F(2)#1, and the other three are terminally bound. The longest As–F bond is observed for the μ_3-F atom, whereas the As–μ_2–F bonds are unexpectedly shorter than those of the terminally bound F atoms.

The overall coordination number of the Cl atom is 2+4, with a distorted octahedral arrangement of the ligands. The Cl atom is displaced from the center of the coordination polyhedron, which is of course due to the unequal Cl–O and Cl···F distances, see above. When the Cl···μ–F contacts are considered, isolated columns, which are arranged along the *c* axis, are obtained (Figure 4). The crystal structure can then be described with the Niggli formula $_\infty^1\left[\langle ClF_{\frac{2}{2+1}}F_{\frac{2}{1+1}}O_{\frac{2}{1}}\rangle\langle AsF_{\frac{1}{1+2}}F_{\frac{2}{1+1}}F_{\frac{3}{1}}\rangle\right]$. The homologous [$BrO_2$][$AsF_6$] salt, in contrast, forms a layer structure.[45]

An analysis of the packing motif shows that a consideration of Cl···Cl distances of *circa* 4.56 to 5.49 Å leads to a distorted octahedron as the coordination polyhedron for the Cl atom. When As···As distances of approximately 4.83 to 6.77 Å are taken into account, a bicapped cube (BCCU-10) is obtained as the coordination polyhedron for the As atom.[65] For Cl···As distances of *circa* 4.00 to 5.41 Å, a distorted or severely distorted cube is obtained as a coordination polyhedron around the As or Cl atoms, respectively, with similar arrangements as the Cs and Cl atoms in the CsCl structure type.[66]

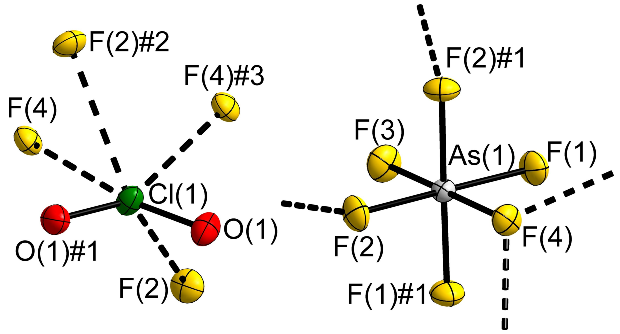

Figure 3. The coordination environment of the Cl and As atom in the crystal structure of [ClO_2][AsF_6]. Short contacts of F atoms belonging to the $[AsF_6]^-$ anions with neighboring Cl atoms are shown as dashed bonds. Symmetry transformations (left): #1 1−*x*, *y*, 1−*z*; #2 1/2−*x*, 1/2+*y*, −*z*; #3 1/2−*x*, 1/2+*y*, 1−*z*. Symmetry transformation (right): #1 *x*, 1−*y*, *z*. Displacement ellipsoids are shown at the 70% probability level at 100 K.

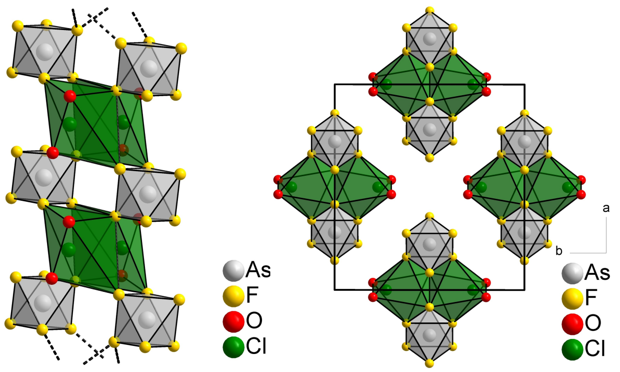

Figure 4. Sections of the crystal structure of [ClO_2][AsF_6]. Coordination polyhedra of Cl atoms are shown in green and those of As atoms in grey. Short contacts of F atoms belonging to the $[PF_6]^-$ anions with neighboring Cl atoms are shown as dashed bonds. Atoms are shown isotropic with arbitrary radii.

The crystal structure of [ClO_2][IrF_6]

Dioxychloronium(V) hexafluoridoiridate(V) crystallizes in the monoclinic space group *P*12/*n*1 (No. 13) with two formula units per unit cell, Pearson code *mP*20, and Wyckoff sequence 13.g^4fe. The compound is, as are [ClO_2][SbF_6] and [BrO_2][SbF_6], isotypic to [ClO_2][RuF_6].[43] Selected crystallographic data and details of the structure determination are given in Table 1. Atomic coordinates, equivalent isotropic and anisotropic displacement parameters are reported in the Supporting Information. The Cl(1) atom occupies the Wyckoff position 2 *f* (site symmetry 2) and is surrounded by the oxygen atoms O(1) and O(1)#1 (Figure 5). The Cl–O bond length is 1.409(3) Å and the O–Cl–O angle is 118.3(2)°. The Ir(1) atom occupies the Wyckoff position 2*e* (site

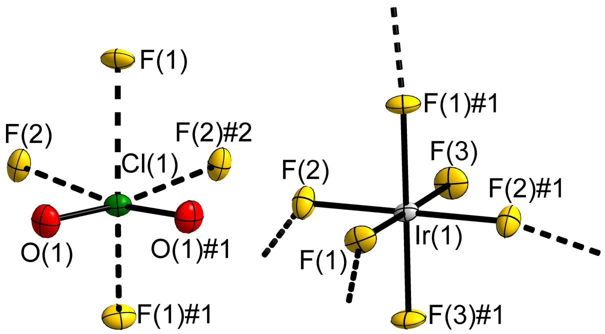

Figure 5. The coordination environment of the Cl(1) and Ir(1) atom in the crystal structure of [ClO_2][IrF_6]. Short contacts of F atoms belonging to the $[IrF_6]^-$ anions with neighboring Cl atoms are shown as dashed bonds. Symmetry transformations (left): #1 3/2−*x*, *y*, 1/2−*z*; #2 1/2+*x*, 1−*y*, −1/2+*z*. Symmetry transformation (right): #1 3/2−*x*, *y*, 3/2−*z*. Displacement ellipsoids are shown at the 70% probability level at 100 K.

symmetry 2) and is surrounded by six F atoms, giving the $[IrF_6]^-$ anion. The Ir–F bond lengths lie in the range of 1.868(2) to 1.892(2) Å and are comparable to those in $Li[IrF_6]$, which are 1.875 Å at room temperature.[67] Three of the six F atoms are terminally bound and the other three are μ-bridging to Cl atoms, which results in an elongation of the Ir–μ–F bond.

The consideration of Cl⋯μ–F contacts leads for the Cl atom to coordination number 2+4 with a distorted octahedral ligand arrangement. The Cl atom is again, see above, displaced from the center of the coordination polyhedron. A layer motif with layers parallel to the *ac* plane is obtained if Cl⋯μ–F contacts are taken into account (Figure 6). The crystal structure can be described with the Niggli formula $_{\infty}^{2}\left[\langle ClF_{\frac{4}{1+1}}O_{\frac{2}{1}}\rangle\langle IrF_{\frac{4}{1+1}}F_{\frac{2}{1}}\rangle\right]$. The Cl and Ir atoms both form a pseudo-cubic primitive lattice and are similarly arranged as the Cs and Cl atoms in the CsCl structure type, with Cl⋯Ir distances of *circa* 4.11 to 5.0 Å.[66]

The crystal structure of $[ClO_2][SnF_{2/2}F_{4/1}]$

To the best of our knowledge, there are thus far no previously reported crystal structures of salts with a pentafluoridostannate(IV) anion, $[SnF_5]^-$. The latter forms one-dimensional infinite strands that can be described with the Niggli formula $_{\infty}^{1}[SnF_{2/2}F_{4/1}]^-$. In contrast, the molecular hexafluoridostannate(IV) anion, $[SnF_6]^{2-}$, was structurally characterized by single-crystal X-ray diffraction in a multitude of salts, such as with alkali metal cations.[68,69] The structures of $[SnF_5]^-$ anions in the $[NF_4]^+$, $[N_2F_3]^+$, and $[N_5]^+$ salts were previously derived from vibrational and/or ^{19}F NMR spectroscopy in the solid-state or solution, respectively.[70–72] Only crystal structures with discrete $[SiF_5]^-$ anions have been reported for the homologous pentafluoridosilicate(IV) anion.[73–76] Whereas the homologous pentafluoridogermanate(IV) anion can either be discrete, as a $[GeF_5]^-$ anion in the 1,3-bis(2,6-diisopropylphenyl)imidazolium salt or a $[Ge_3F_{16}]^{4-}$ anion in $[C(NH_2)_2NH_3]_2[Ge_3F_{16}]\cdot n HF$ ($n=1$, 2), or "polymerize" to form the $_{\infty}^{1}\left[GeF_{2/2}F_{4/1}\right]^-$ anion.[42,77,78] The $[GeF_6]$ polyhedra in the latter can either be *trans*-bridged to a linear chain as in $[XeF_5][GeF_{2/2}F_{4/1}]$ or *cis*-bridged to helical chains as in $[ClO_2][GeF_{2/2}F_{4/1}]$ or $O_2[GeF_5]\cdot HF$.[42,78] For the Sn system, anions with higher Sn content such as $[Sn_2F_9]^-$ and $[Sn_5F_{24}]^{4-}$ were described and they were either characterized by vibrational spectroscopy or single-crystal X-ray diffraction.[78–80] The $[Sn_2F_9]^-$ anion shows a ladder-like structure motif in $O_2[Sn_2F_9]$ and a more complex layer-structure with hexa- and hepta-coordinated Sn(IV) atoms in $O_2[Sn_2F_9]\cdot 0.9HF$.[78] Similar coordination numbers are observed for the Sn(IV) atoms in $[XeF_5]_4[Sn_5F_{24}]$, in which the anion also forms a layer-motif.[80]

Dioxychloronium(V) pentafluoridostannate(V) crystallizes in the monoclinic space group $P12_1/n1$ (No. 14) with four formula units per unit cell, Pearson code *mP*36, and Wyckoff sequence 14.e^9. Selected crystallographic data and details of the structure determination are given in Table 1. Atomic coordinates, equivalent isotropic and anisotropic displacement parameters are reported in the Supporting Information. The Cl(1) atom occupies the Wyckoff position 4*e* (site symmetry 1) and is surrounded by the oxygen atoms O(1) and O(2), forming the $[ClO_2]^+$ cation (Figure 7).

The Cl–O bond lengths are 1.4045(13) and 1.4050(18) Å and the O–Cl–O angle is 117.37(10)°. The Sn(1) atom also occupies the Wyckoff position 4*e* and is surrounded by six F atoms in the shape of a distorted octahedron. The Sn–F bond lengths lie in the range of 1.9047(13) to 2.0627(13) Å. Two of the F atoms, F(1) and F(1)#1, are μ-bridging between Sn atoms, giving the $_{\infty}^{1}\left[SnF_{2/2}F_{4/1}\right]^-$ anion. The anion is a linear zig-zag chain formed by *cis*-bridged $[SnF_6]$ polyhedra (Figure 8). The F atoms F(2) to F(4) show short contacts with the Cl(1) atom with Cl⋯μ–F

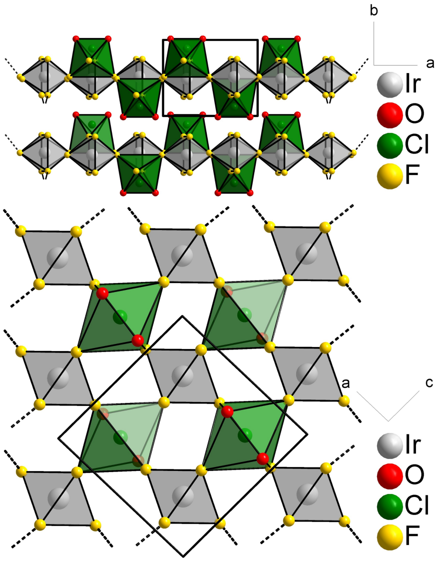

Figure 6. Crystal structure of $[ClO_2][IrF_6]$ projected along the *c* (top) or *b* (bottom) axis. Coordination polyhedra of Cl atoms are shown in green and those of Ir atoms in grey. Short contacts of F atoms belonging to the $[IrF_6]^-$ anions with neighboring Cl atoms are shown as dashed bonds. Atoms are shown as isotropic with arbitrary radii.

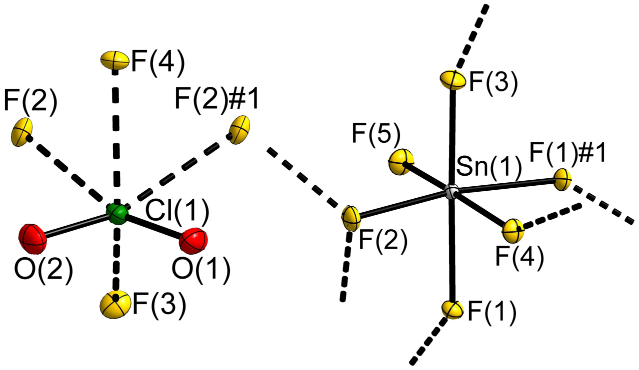

Figure 7. Cl and Sn atom environments in the crystal structure of $[ClO_2][SnF_{2/2}F_{4/1}]$. Short contacts of F atoms belonging to the $_{\infty}^{1}\left[SnF_{2/2}F_{4/1}\right]^-$ anions with neighboring Cl atoms are shown as dashed bonds. The atoms F(1) and F(1)#1 are μ-bridging between Sn atoms and their contacts are also shown as dashed bonds. Symmetry transformation (left): #1 1−*x*, 1−*y*, 1−*z*. Symmetry transformation (right): #1 1/2−*x*, 1/2+*y*, 1/2−*z*. Displacement ellipsoids are shown at the 70% probability level at 100 K.

distances of 2.3847(14) to 2.6912(14) Å, whereas the F(2) atom is bridging to two Cl atoms and is thus μ_3-bridging. As in the previously described compounds, the Cl atom has the coordination number 2+4 and is surrounded by the ligands in a distorted octahedral manner. When the Cl⋯μ–F contacts are taken into account, a layer structure is obtained with layers in the (101)-plane, best described with the Niggli formula $_\infty^{\;2}\left[\langle \mathrm{ClF}_{\frac{2}{2+1}}\mathrm{F}_{\frac{2}{1+1}}\mathrm{O}_{\frac{2}{1}}\rangle\langle \mathrm{SnF}_{\frac{1}{1+2}}\mathrm{F}_{\frac{2}{1+1}}\mathrm{F}_{\frac{2}{2}}\mathrm{F}_{\frac{1}{1}}\rangle\right]$.

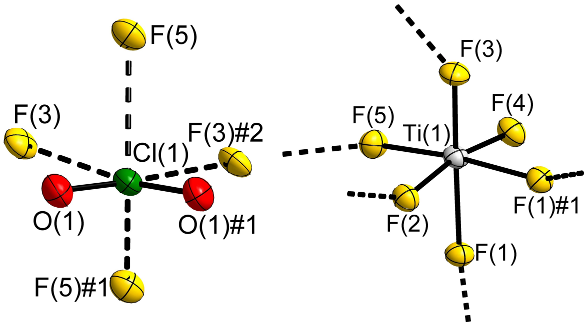

Figure 9. Cl and Ti atom environments in the crystal structure of $[\mathrm{ClO_2}][[\mathrm{TiF_{3/2}F_{3/1}}]_2]$. Short contacts of F atoms belonging to the $_\infty^{\;1}\left[[\mathrm{TiF_{3/2}F_{3/1}}]_2\right]^-$ anions with neighboring Cl atoms are shown as dashed bonds (left). The atoms F(1), F(1)#1, and F(2) are μ_2-bridging between Ti atoms and these contacts are shown as dashed bonds (right). Symmetry transformations (left): #1 1−*x*, *y*, 1/2−*z*, #2 1−*x*, *y*, 3/2−*z*. Symmetry transformation (right): #1 *x*, 1−*y*, 1/2+*z*. Displacement ellipsoids are shown at the 70 % probability level at 100 K.

The crystal structure of $[\mathrm{ClO_2}][[\mathrm{TiF_{3/2}F_{3/1}}]_2]$

Dioxychloronium(V) nonafluoridodititanate(IV) crystallizes in the monoclinic space group *C*2/*c* (No. 15) with four formula units per unit cell, Pearson code *mS*56, and Wyckoff sequence $15.f^6e^2$. Selected crystallographic data and details of the structure determination are given in Table 1. Atomic coordinates, equivalent isotropic and anisotropic displacement parameters are reported in the Supporting Information. The Cl(1) atom occupies Wyckoff position 4*e* (site symmetry 2) and is surrounded by the oxygen atoms O(1) and O(2)#1, giving a $[\mathrm{ClO_2}]^+$ cation with a Cl–O bond length of 1.401(3) Å and an O–Cl–O angle of 118.7(2)° (Figure 9). The Ti(1) atom occupies the general position 8*f* and is surrounded by six F atoms in the shape of a distorted octahedron with Ti−F bond lengths of 1.776(2) to 1.980(2) Å.

Three of the F atoms, F(1), F(1)#1, and F(2), are μ-bridging between Ti atoms, resulting in the formation of the ladder-like anion running along the *c* axis with corner-sharing $[\mathrm{TiF_6}]$ polyhedra, via "facial" F atoms (Figure 10). The anion can be described with the Niggli formula $_\infty^{\;1}\left[[\mathrm{TiF_{3/2}F_{3/1}}]_2\right]^-$. The structural chemistry of fluoridotitanates(IV) is rich and many different structural motifs have been described.[81] The simplest discrete anion of the fluoridotitanates(IV) is the $[\mathrm{TiF_6}]^{2-}$ anion, which has been observed in the crystal structures of salts such as $A^{\mathrm{I}}_2[\mathrm{TiF_6}]$ (A^{I}=Li – Cs) and $A^{\mathrm{II}}[\mathrm{TiF_6}]$ (A^{II}=Ag, Ca, Sr, Ba).[82–87] All other fluoridotitanate(IV) anions are derived from $[\mathrm{TiF_6}]$ polyhedra by condensation and thus corner- or edge-sharing of such polyhedra is present. The structure motifs range from discrete anions as in $[\mathrm{TiF_2}([15]\mathrm{crown}\text{-}5)][\mathrm{Ti_4F_{18}}]\cdot 0.5\mathrm{CH_3CN}$, $[\mathrm{XeF_5}][\mathrm{Ti_4F_{19}}]$ and $\mathrm{K_4}[\mathrm{Ti_8F_{36}}]\cdot 8\mathrm{HF}$, to one-dimensional chains or strands as in $\mathrm{K}[\mathrm{TiF_5}]$ and $\mathrm{Rb}[\mathrm{Ti_2F_9}]$, and even to a layer structure in $\mathrm{Cs}[\mathrm{Ti_8F_{33}}]$.[82,88–91] Compounds with similarly shaped $[\mathrm{Ti_2F_9}]^-$ anions were described previously for the salts $A[\mathrm{Ti_2F_9}]$ (A=Rb, Cs, $\mathrm{H_3O}$, $\mathrm{C_3H_5N_2}$).[82,92,93] The Ti−F bond lengths in $\mathrm{Na}[\mathrm{Ti_2F_9}]\cdot\mathrm{HF}$ are 1.768(2)–1.974(1) Å at 200 K and in $\mathrm{Rb}[\mathrm{Ti_2F_9}]$ they are 1.762(2)–2.005(2) Å at 157 K.[82]

Two of the F atoms, F(3) and F(5), show short contacts to the Cl atom with Cl⋯μ–F distances of 2.665(2) and 2.708(2) Å. When the Cl⋯μ–F contacts are taken into account, the coordination number 2+4 results for the Cl atom with a distorted octahedral arrangement of the ligands. The Cl⋯μ–F interaction leads to a columnar structure along the *c* axis that

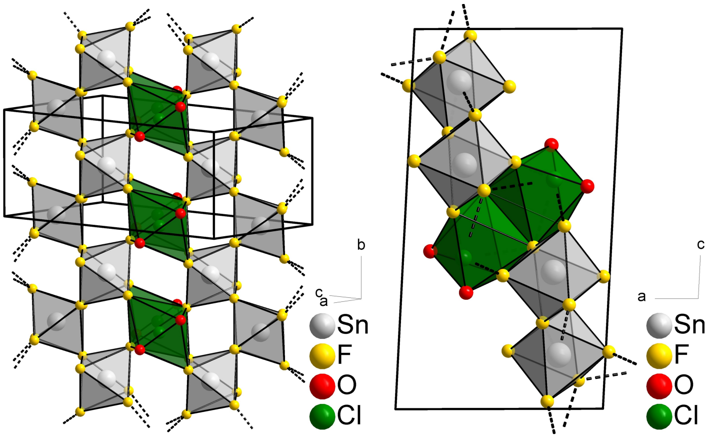

Figure 8. Crystal structure of $[\mathrm{ClO_2}][\mathrm{SnF_{2/2}F_{4/1}}]$, with the layer motif shown on the left and a side view of a layer on the right. Coordination polyhedra of the Cl atoms are shown in green and those of Sn atoms in grey. Short contacts of F atoms belonging to the $_\infty^{\;1}\left[\mathrm{SnF_{2/2}F_{4/1}}\right]^-$ anions with neighboring Cl atoms and to further Sn atoms are shown as dashed bonds. Atoms are shown as isotropic with arbitrary radii.

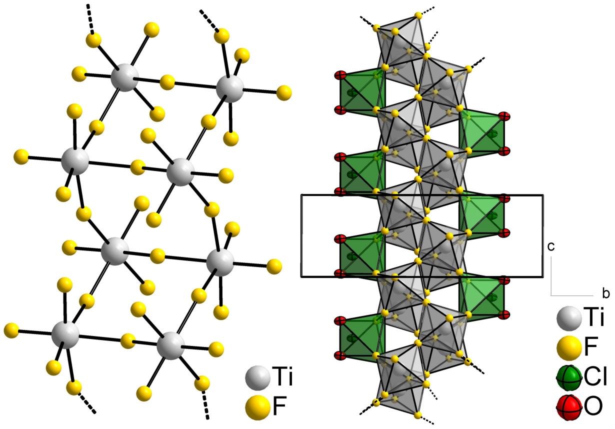

Figure 10. Crystal structure of $[ClO_2][[TiF_{3/2}F_{3/1}]_2]$. The ${}_{\infty}^{1}\left[\left[TiF_{3/2}F_{3/1}\right]_2\right]^-$ anion is shown on the left and the column obtained from the Cl···μ–F contacts on the right. Coordination polyhedra of Cl atoms are shown in green and those of Ti atoms in grey. Short contacts of F atoms belonging to the ${}_{\infty}^{1}\left[\left[TiF_{3/2}F_{3/1}\right]_2\right]^-$ anions with the neighboring Cl atoms and to further Ti atoms are shown as dashed bonds. Atoms are shown isotropic with arbitrary radii.

can be described with the Niggli formula ${}_{\infty}^{1}\left[\langle ClF_{\frac{4}{1+1}}O_{\frac{2}{1}}\rangle\langle TiF_{\frac{2}{1+1}}F_{\frac{3}{2}}F_{\frac{1}{1}}\rangle_2\right]$ (Figure 10).

The crystal structure of $[ClO_2][Nb_3F_{16}]$

It is well-known that pentafluorides, MF_5 (M = e.g. As, Sb, Bi), can react with fluoride ion donors, such as AF, to give anions with higher nuclearity than $[MF_6]^-$ if appropriate ratios of AF and MF_5 are chosen for the reaction.[94] These bi- and polymetallic complex anions can be described with the formula $[M_nF_{5n+1}]^-$ (n = 2, 3, 4) and can be considered as weakly coordinating anions, but not all anions are known for each pentafluoride.[94,95] For actinide pentafluorides no anions of the form $[M_nF_{5n+1}]^-$ (n = 2, 3, 4) have been reported as of yet, and these pentafluorides might differ in their reactivity and structural chemistry from main group and transition metal pentafluorides due to the higher possible coordination number for the central atom.[96] For example, in the compound $Sr[U_2F_{12}]$, the $[U_2F_{12}]^{2-}$ anion may be described as two condensed $[UF_6]^-$ anions, resulting in coordination number seven for the U atoms.[97]

The best-studied AF/MF_5 system is probably that of SbF_5, for which crystal structures of compounds containing all above-mentioned anions have been described.[94,98–100] In the crystal structures with the anions $[Sb_3F_{16}]^-$ and $[Sb_4F_{21}]^-$ almost exclusively *cis*-bridging central $[SbF_6]$ polyhedra are observed.[94,98,100] The only example of a *trans*-bridging central $[SbF_6]$ polyhedron seems to be $Br_2[Sb_3F_{16}]$.[101]

In contrast to that, the NbF_5 system is less studied and only the $[Nb_2F_{11}]^-$ anion was characterized by single-crystal diffraction.[102–104] Reports on the AF/NbF_5 system (A = Rb, Cs, Tl) exist. It was investigated by powder X-ray diffraction and differential thermal analysis and it was assumed that compounds of the composition $A[Nb_3F_{16}]$ (A = Rb, Tl) and $Cs[Nb_4F_{21}]$ form.[105]

Dioxychloronium(V) hexadecafluoridotriniobate(V) crystallizes in the monoclinic space group $C2/c$ (No. 15) with four formula units per unit cell, Pearson code *mS*88, and Wyckoff sequence 15.$f^{10}e^2$. Selected crystallographic data and details of the structure determination are given in Table 1. Atomic coordinates, equivalent isotropic and anisotropic displacement parameters are reported in the Supporting Information. The Cl(1) atom occupies the Wyckoff position 4*e* (site symmetry 2) and is surrounded by the oxygen O(1) and O(1)#1 giving a $[ClO_2]^+$ cation with a Cl–O bond length of 1.4084(6) Å and an O–Cl–O angle of 119.06(5)°(Figure 11).

The two symmetry-independent Nb atoms, Nb(1) and Nb(2), occupy the Wyckoff positions 8*f* and 4*e* (site symmetries 1 and 2), respectively. Each of the Nb atoms is surrounded by six fluorine atoms, of which F(1) and F(1)#1 are μ-bridging between Nb atoms. The resulting $[Nb_3F_{16}]^-$ anion consists of a *cis*-bridging central $[NbF_6]$ polyhedron and can be described with

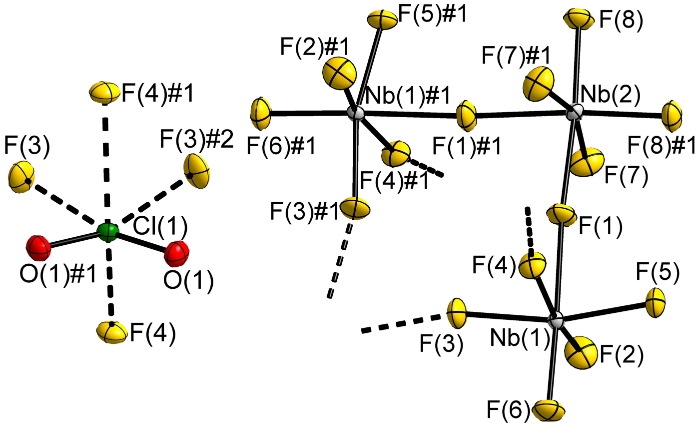

Figure 11. Cl and Nb atoms environments in the crystal structure of $[ClO_2][Nb_3F_{16}]$. Short contacts of F atoms belonging to the $[Nb_3F_{16}]^-$ anions with neighboring Cl atoms are shown as dashed bonds. Symmetry transformations (left): #1 $1-x$, y, $1/2-z$; #2 $1-x$, y, $1/2-z$. Symmetry transformation (right): #1 $1-x$, y, $3/2-z$. Displacement ellipsoids are shown at the 70% probability level at 100 K.

the Niggli formula ${}_{\infty}^{0}\left[\langle \mathrm{NbF}_{\frac{1}{2}}\mathrm{F}_{\frac{5}{1}}\rangle_2\langle \mathrm{NbF}_{\frac{2}{2}}\mathrm{F}_{\frac{4}{1}}\rangle\right]^-$. The Nb–F bond lengths lie in the range of 1.8183(5) to 1.9011(5) Å for terminally bound F atoms and 2.0298(5) and 2.1082(5) Å for the μ-bridging F atoms. They agree with previously reported Nb–F bond lengths for $[2,4\text{-(OMe)}_2\mathrm{C}_6\mathrm{H}_5][\mathrm{Nb}_2\mathrm{F}_{11}]$, which are 1.857(2) to 1.872(3) Å for the terminal and 2.0584(5) Å for the μ-bridging F atom at 100 K.[104] In comparison to $[\mathrm{Sb}_3\mathrm{F}_{16}]^-$ salts with cations such as Cs^+, $[\mathrm{Cl}_3]^+$ $[\mathrm{OCNCO}]^+$ or $[\mathrm{C}_{10}\mathrm{Cl}_{10}]^+$, in which the Sb–μ–F–Sb angles differ significantly from 180° and the $[\mathrm{SbF}_6]$ polyhedra are tilted against each other, the Nb–μ–F–Nb angle in $[\mathrm{ClO}_2][\mathrm{Nb}_3\mathrm{F}_{16}]$ is close to 180° with 175.13(3)° and the $[\mathrm{NbF}_6]$ polyhedra are not tilted against each other.[98,106–108] This might be caused by the coordination number six of the Cl atom and the shape of the formed $[\mathrm{ClO}_2\mathrm{F}_4]$ polyhedron, see below.

Two of the F atoms, F(3) and F(4) atoms show short contacts to the Cl atom with Cl⋯μ–F distances of 2.4904(5) and 2.6554(6) Å. If these Cl⋯μ–F contacts are considered, the Cl atom is coordinated by $2+4$ ligands in the shape of a distorted octahedron. Then, a ladder-like structure motif with interconnected $[\mathrm{ClO}_2[\mathrm{Nb}_3\mathrm{F}_{16}]]$ units running along the *c* axis is obtained, with a $[\mathrm{ClO}_2]^+$ cation coordinated by three $[\mathrm{Nb}_3\mathrm{F}_{16}]^-$ anions (Figure 12). The overall structure can then be described with the Niggli formula ${}_{\infty}^{1}\left[\langle \mathrm{ClF}_{\frac{4}{1+1}}\mathrm{O}_{\frac{2}{1}}\rangle\langle \mathrm{NbF}_{\frac{2}{1+1}}\mathrm{F}_{\frac{1}{2}}\mathrm{F}_{\frac{3}{1}}\rangle_2\langle \mathrm{NbF}_{\frac{2}{2}}\mathrm{F}_{\frac{4}{1}}\rangle\right]$.

The crystal structure of $[\mathrm{ClO}_2][\mathrm{Mo}_3\mathrm{O}_3\mathrm{F}_{13}]$

Dioxychloronium(V) tridecafluoridotrioxidotrimolybdate(VI) crystallizes in the triclinic space group $P\bar{1}$ (No. 2) with two formula units per unit cell, Pearson code *aP*44 and Wyckoff sequence $2.i^{22}$. Selected crystallographic data and details of the structure determination are given in Table 3. Atomic coordinates, equivalent isotropic and anisotropic displacement parameters are reported in the Supporting Information. The Cl(1) atom occupies the general 2*i* position and is surrounded by the oxygen atoms O(1) and O(2), giving the $[\mathrm{ClO}_2]^+$ cation, see Figure 13. The Cl–O bond lengths are 1.3950(18) and 1.4068(18) Å and the O–Cl–O angle is 119.65(10)°.

Three symmetry-independent Mo atoms are present, Mo(1) to Mo(3), which are each surrounded by one oxygen atom, and five fluorine atoms in the shape of a distorted octahedron. With a central *cis*-bridging $[\mathrm{MoOF}_5]$ polyhedron, two of the F atoms, F(5) and F(9), are μ-bridging between the other two Mo atoms, resulting in the $[\mathrm{Mo}_3\mathrm{O}_3\mathrm{F}_{13}]^-$ anion that can be described with the Niggli formula ${}_{\infty}^{0}\left[\langle \mathrm{MoF}_{\frac{1}{2}}\mathrm{F}_{\frac{4}{1}}\mathrm{O}_{\frac{1}{1}}\rangle_2\langle \mathrm{MoF}_{\frac{2}{2}}\mathrm{F}_{\frac{3}{1}}\mathrm{O}_{\frac{1}{1}}\rangle\right]^-$ (Figure 13). Molybdenum oxide tetrafluoride, MoOF_4, can also form other anions of different nuclearity with fluoride ion donors, such as the mononuclear $[\mathrm{MoOF}_5]^-$ and the dinuclear $[\mathrm{Mo}_2\mathrm{O}_2\mathrm{F}_9]^-$ anion.[109,110]

The Mo–O bond lengths lie in the range of 1.6435(17) to 1.6457(17) Å and the Mo–F bond lengths for terminally bound F atoms in the range of 1.8196(13) to 1.9288(13) Å and 2.1071(13) to 2.3161(13) Å for the μ–F atoms. They agree with the previously reported bond lengths for $[\mathrm{Cl}_2\mathrm{BrO}_6][\mathrm{Mo}_3\mathrm{O}_3\mathrm{F}_{13}]$, which are 1.652(2)–1.662(2) Å (Mo–O), 1.819(2)–1.949(2) Å (Mo–F), and 2.102(2)–2.249(2) Å (Mo–μ–F) at 100 K.[45]

The $[\mathrm{Mo}_3\mathrm{O}_3\mathrm{F}_{13}]^-$ anion can also be thought of as a $[\mathrm{Mo}_2\mathrm{O}_2\mathrm{F}_9]^-$ anion that coordinates via the F(9) atom to a MoOF_4 unit. This becomes evident, as the Mo(3)–F(9) bond of 2.3161(13) Å is significantly longer than the Mo(1)–F(5) and Mo(2)–F(5) bonds of 2.1112(13) and 2.1071(13) Å, respectively. The latter nicely agree with the Mo–μ–F bond lengths in the alkali metal salts $A[\mathrm{Mo}_2\mathrm{O}_2\mathrm{F}_9]$ ($A=$ Li–Cs).[110]

Three of the F atoms of the anion, F(1), F(2), and F(11), show short contacts to the Cl atom with Cl⋯μ–F distances of 2.4617(15) to 2.9054(15) Å. In total, the Cl atom is then surrounded by six ligands in the form of a distorted octahedron. If the Cl⋯μ–F contacts are considered, a dimer of the form $[[\mathrm{ClO}_2][\mathrm{Mo}_3\mathrm{O}_3\mathrm{F}_{13}]]_2$ that can also be described with the Niggli formula ${}_{\infty}^{0}\left[\left[\langle \mathrm{ClF}_{\frac{4}{1+1}}\mathrm{O}_{\frac{2}{1}}\rangle\langle \mathrm{MoF}_{\frac{2}{1+1}}\mathrm{F}_{\frac{1}{2}}\mathrm{F}_{\frac{2}{1}}\mathrm{O}_{\frac{1}{1}}\rangle\langle \mathrm{MoF}_{\frac{2}{2}}\mathrm{F}_{\frac{3}{1}}\mathrm{O}_{\frac{1}{1}}\rangle\langle \mathrm{MoF}_{\frac{1}{1+1}}\mathrm{F}_{\frac{1}{2}}\mathrm{F}_{\frac{3}{1}}\mathrm{O}_{\frac{1}{1}}\rangle\right]_2\right]$ is ob-

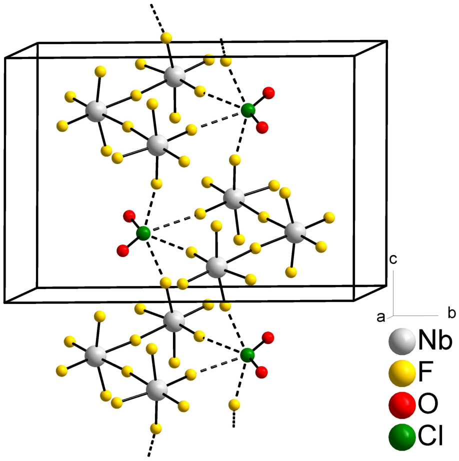

Figure 12. Section of the crystal structure of $[\mathrm{ClO}_2][\mathrm{Nb}_3\mathrm{F}_{16}]$. Short contacts of F atoms belonging to the $[\mathrm{Nb}_3\mathrm{F}_{16}]^-$ anions with neighboring Cl atoms are shown as dashed bonds. Atoms are shown isotropic with arbitrary radii.

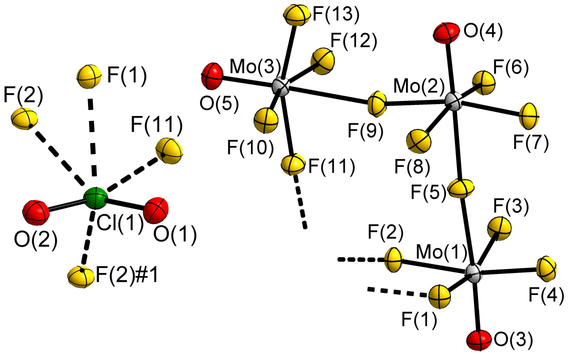

Figure 13. Cl and Mo atoms environments in the crystal structure of $[\mathrm{ClO}_2][\mathrm{Mo}_3\mathrm{O}_3\mathrm{F}_{13}]$. Short contacts of F atoms belonging to the $[\mathrm{Mo}_3\mathrm{O}_3\mathrm{F}_{13}]^-$ anions with neighboring Cl atoms are shown as dashed bonds. Symmetry transformation: #1 $1-x$, $1-y$, $1-z$. Displacement ellipsoids are shown at the 70 % probability level at 100 K.

Table 3. Selected crystallographic data and details of the structure determinations of $[ClO_2][Mo_3O_3F_{13}]$ and $[ClO_2][Re_3O_6F_{10}]$.

Compound	$[ClO_2][Mo_3O_3F_{13}]$	$[ClO_2][Re_3O_6F_{10}]$
Molar mass [$g \cdot mol^{-1}$]	650.27	912.05
Space group (No.)	$P\bar{1}$(2)	$P\bar{1}$(2)
a [Å]	7.8633(5)	8.6351(5)
b [Å]	8.8097(6)	8.9888(6)
c [Å]	10.1029(7)	9.0785(6)
α [°]	73.285(5)	113.872(2)
β [°]	84.923(5)	96.647(2)
γ [°]	68.553(5)	98.259(2)
V [$Å^3$]	623.77(8)	625.82(7)
Z	2	2
Pearson symbol	$aP44$	$aP44$
$\rho_{calc.}$ [$g \cdot cm^{-3}$]	3.46	4.84
μ [mm^{-1}]	3.370	29.323
Color	colorless	colorless
Crystal morphology	block	block
Crystal size [mm^3]	0.17 × 0.19 × 0.20	0.07 × 0.10 × 0.16
T [K]	100	
λ [Å]	0.71073 (Mo–K_α)	
No. of reflections	13712	54494
θ range [°]	2.11–32.58	2.43–33.47
Range of Miller indices	$-11 \leq h \leq 11$ $-13 \leq k \leq 13$ $-15 \leq l \leq 15$	$-13 \leq h \leq 12$ $-13 \leq k \leq 13$ $-13 \leq l \leq 13$
Absorption correction	integration	multi-scan
$Trans._{max}$, $Trans._{min}$	0.66, 0.51	0.38, 0.09
R_{int}, R_σ	0.0420, 0.0523	0.0548, 0.0371
Completeness of the data set	0.998	0.941
No. of unique reflections	4537	4604
No. of parameters	199	199
No. of restraints	0	0
No. of constraints	0	0
S (all data)	0.964	0.973
$R(F)$ ($I \geq 2\sigma(I)$, all data)	0.0245, 0.0345	0.0253, 0.0342
$wR(F^2)$ ($I \geq 2\sigma(I)$, all data)	0.0504, 0.0525	0.0500, 0.0517
Extinction coefficient	not refined	not refined
$\Delta\rho_{max}$, $\Delta\rho_{min}$ [$e \cdot Å^{-3}$]	0.88, −1.17	2.44, −2.77

tained (Figure 14). One of the dimers is surrounded by twelve further dimers in a cuboctahedron-like manner, and therefore the compound is related to the Cu structure type.[111]

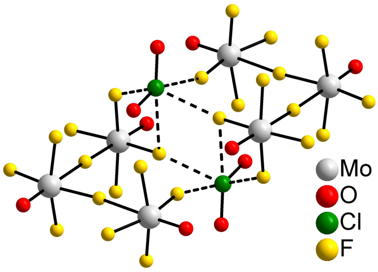

Figure 14. Dimer of $[ClO_2][Mo_3O_3F_{13}]$, which is obtained by taking the Cl⋯μ–F contacts into account. Atoms are shown as isotropic with arbitrary radii.

The crystal structure of $[ClO_2][Re_3O_6F_{10}]$

Dioxychloronium(V) decafluoridohexaoxidotrirhenate(VII) crystallizes with two formula units per unit cell in the triclinic space group $P\bar{1}$ (No. 2), Pearson code $aP44$ and Wyckoff sequence $2.i^{22}$. Selected crystallographic data and details of the structure determination are given in Table 3. Atomic coordinates, equivalent isotropic and anisotropic displacement parameters are reported in the Supporting Information. The Cl(1) atom occupies the general $2i$ position and is surrounded by the oxygen atoms O(1) and O(2), giving the $[ClO_2]^+$ cation, see Figure 15. The Cl–O bond lengths are 1.384(4) and 1.418(4) Å and the O–Cl–O angle is 118.9(2)°.

There are three symmetry-independent Re atoms present, Re(1) to Re(3), which are each surrounded by four F and two O atoms. Two of the F atoms are μ-bridging between Re atoms, resulting in the $[Re_3O_6F_{10}]^-$ anion. This anion contains a central *cis*-bridging $[ReO_2F_4]$ polyhedron and can also be described with the Niggli formula $_\infty^0\left[\langle ReF_{\frac{1}{2}}F_{\frac{3}{1}}O_{\frac{2}{1}}\rangle_2\langle ReF_{\frac{2}{2}}F_{\frac{2}{1}}O_{\frac{2}{1}}\rangle\right]^-$. The Re–O bond lengths lie in the range of 1.652(3) to 1.692(3) Å, and the Re–F bond lengths range from 1.858(3) to 1.935(3) Å for the terminal and from 2.051(3) to 2.179(3) Å for the bridging F atoms. They agree with the reported bond lengths for Cs$[Re_3O_6F_{10}]$ which are 1.669(8) to 1.715(8) for Re–O, 1.848(6) to 1.936(7) for Re–F, and 2.039(6) to 2.213(6) Å for Re–μ–F, at 155 K.[112]

doi.org/10.1002/ejic.202000908

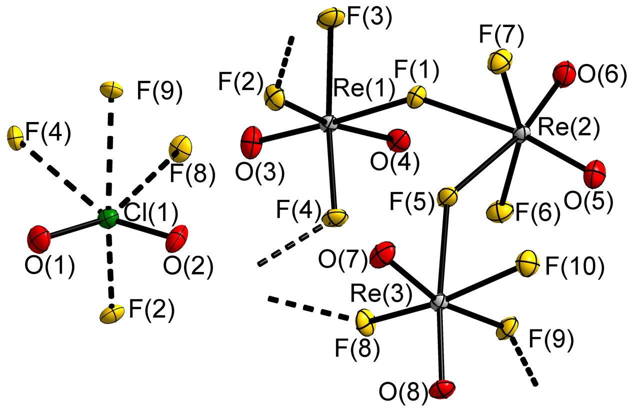

Figure 15. Cl and Re atoms environments in the crystal structure of $[ClO_2][Re_3O_6F_{10}]$. Short contacts of F atoms belonging to the $[Re_3O_6F_{10}]^-$ anions with neighboring Cl atoms are shown as dashed bonds. Displacement ellipsoids are shown at the 70 % probability level at 100 K.

Four of the F atoms, F(2), F(4), F(8) and F(9), show short contacts to the Cl atom with Cl⋯μ–F distances of 2.354(3) to 2.749(3) Å. The resulting coordination number for the Cl atom is 2+4 and its coordination sphere is distorted octahedral. Overall, a column-like structure motif running along the *a* axis is obtained considering these Cl⋯μ–F interactions. The crystal structure can be described with the Niggli formula ${}_{\infty}^{1}\left[\langle ClF_{\frac{4}{1+1}}O_{\frac{2}{1}}\rangle\langle ReF_{\frac{2}{1+1}}F_{\frac{1}{2}}F_{\frac{1}{1}}O_{\frac{2}{1}}\rangle_{2}\langle ReF_{\frac{2}{2}}F_{\frac{2}{1}}O_{\frac{2}{1}}\rangle\right]$ (Figure 16).

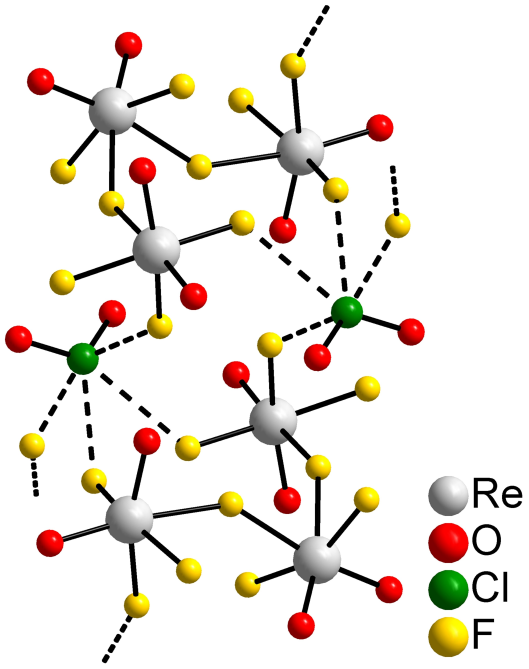

Figure 16. Section of the crystal structure of $[ClO_2][Re_3O_6F_{10}]$. Short contacts of F atoms belonging to the $[Re_3O_6F_{10}]^-$ anions with neighboring Cl atoms are shown as dashed bonds. Atoms are shown isotropic with arbitrary radii.

Quantum-chemical calculations

Quantum-chemical solid-state calculations were carried out for the investigated $[ClO_2]^+$ salts with CRYSTAL17 (DFT-PBE0/TZVP level of theory).[113,114] The optimized structures are reported in the Supporting Information and a comparison of experimental and calculated bond lengths, atomic distances, and angles are given in Table 2 and Table 4 (O–Cl–O angles), Table 5 (*M*–O and *M*–F bond lengths), and Table 6 (average atomic charges). The calculated Cl–O bond lengths are ~1.44 Å and similar among the investigated compounds, being approximately 1.6 to 2.6 % larger than the experimentally determined ones. The quantum-chemically calculated Cl⋯μ–F distances are generally shorter and the interaction of the Cl atom with the F atoms seems to be overestimated by the employed level of theory.

To get a qualitative picture of the bonding in these compounds, the atomic charges and overlap populations between atoms were examined by Mulliken population analyses. Average atomic charges are reported in Table 6 and the average overlap populations in Table 7. The atomic charges of the Cl atoms show only minor differences among the compounds. The lowest charge with +1.09 on the Cl atom is calculated for $[ClO_2][Mo_3O_3F_{13}]$ and the highest with +1.20 for $[ClO_2][Nb_3F_{16}]$. The most negatively charged F atoms are the bridging ones, whereas those bridging to the Cl atoms are more negatively charged than those bridging between *M* atoms. The average overlap populations indicate covalent Cl–O bonds and ionic Cl⋯μ–F interactions, which can be expected as the respective distances are quite large. Overall, the impact on the bonding within the $[ClO_2]^+$ cations by the fluoridometallate or oxidofluoridometallate anions is minor.

Raman spectra of $[ClO_2]^+$ compounds

The $[ClO_2]^+$ compounds presented here were furthermore investigated by Raman spectroscopy. An exemplary Raman spectrum of $[ClO_2][AsF_6]$ is shown in Figure 17 and low- and high-resolution Raman spectra of the other salts are reported in the Supporting Information. The Raman spectra were furthermore calculated by quantum-chemical calculations, which are based on the optimized structures. Band assignments for the calculated spectra are given in the Supporting Information.

In previous reports on the vibrational spectra of $[ClO_2]^+$ compounds, the symmetry of the $[ClO_2]^+$ cations was assumed

Table 4. Experimental and calculated O–Cl–O angles in $[ClO_2]^+$ salts.

Compound	∠O–Cl–O [°]	calculated ∠O–Cl–O (DFT-PBE0/TZVP, solid-state) [°]
$[ClO_2][PF_6]$	119.75(5)	117.7
$[ClO_2][AsF_6]$	119.57(11)	116.7
$[ClO_2][IrF_6]$	118.3(2)	116.6
$[ClO_2][SnF_{2/2}F_{4/1}]$	117.37(10)	115.3
$[ClO_2][[TiF_{3/2}F_{3/1}]_2]$	118.7(2)	116.1
$[ClO_2][Nb_3F_{16}]$	119.06(5)	116.5
$[ClO_2][Mo_3O_3F_{13}]$	119.65(10)	117.1
$[ClO_2][Re_3O_6F_{10}]$	118.9(2)	116.5

Table 5. Experimental and calculated *M*–O and *M*–F bond lengths (*M*: central atom of the anion) of fluoridometallate and oxidofluoridometallate anions in $[ClO_2]^+$ salts.

Compound	Bond length [Å]			Calculated bond length (DFT-PBE0/TZVP, solid-state) [Å]		
	M–O	*M*–F (non-bridging)	*M*–F (bridging)	*M*–O	*M*–F (non-bridging)	*M*–F (bridging)
$[ClO_2][PF_6]$	–	1.5881(6)	1.5993(7)–1.6197(6)	–	1.61	1.62–1.65
$[ClO_2][AsF_6]$	–	1.7034(14), 1.7231(9)	1.7208(9), 1.7418(13)	–	1.71	1.73–1.76
$[ClO_2][IrF_6]$	–	1.868(2)	1.873(2), 1.892(2)	–	1.85	1.88, 1.93
$[ClO_2][SnF_{2/2}F_{4/1}]$	–	1.9047(13)	1.9321(13)–1.9336(12), 2.0458(12),[a] 2.0627(13)[a]	–	1.91	1.95–1.96, 2.06[a], 2.08[a]
$[ClO_2][[TiF_{3/2}F_{3/1}]_2]$	–	1.776(2)	1.778(2), 1.787(2), 1.968(1)–1.980(2)[a]	–	1.78	1.79, 1.80, 1.98–1.99[a]
$[ClO_2][Nb_3F_{16}]$	–	1.8183(5)–1.8675(5)	1.8743(5), 1.9011(5), 2.0298(5)[a], 2.1082(5)[a]	–	1.84–1.87	1.90, 1.94, 2.06[a], 2.12[a]
$[ClO_2][Mo_3O_3F_{13}]$	1.6435(17)–1.6457(17)	1.8196(14)–1.8454(13)	1.8699(14)–1.8957(13), 1.9288(13)–2.3161(13)[a]	1.65–1.66	1.84–1.87	1.89–1.93, 1.94–2.33[a]
$[ClO_2][Re_3O_6F_{10}]$	1.652(3)–1.692(3)	1.858(3)–1.875(3)	1.859(3)–1.935(3), 2.051(3)–2.179(3)[a]	1.67–1.68	1.86–1.87	1.88–2.03, 2.12–2.18[a]

[a] μ-Bridging between *M* atoms.

Table 6. Average atomic charges from Mulliken population analyses of the optimized solid-state structures of $[ClO_2]^+$ salts.

Compound	Average atomic charge [*e*]					
	M [a]	Cl	O ($[ClO_2]^+$)	O (Anion)	F (non-bridging)	F (bridging)
$[ClO_2][PF_6]$	1.78	1.15	−0.17	–	−0.41	−0.44
$[ClO_2][AsF_6]$	1.62	1.15	−0.16	–	−0.36	−0.42
$[ClO_2][IrF_6]$	1.70	1.15	−0.22	–	−0.38	−0.42
$[ClO_2][SnF_{2/2}F_{4/1}]$	1.82	1.17	−0.23	–	−0.49	−0.52, −0.49[b]
$[ClO_2][[TiF_{3/2}F_{3/1}]_2]$	1.94	1.18	−0.18	–	−0.49	−0.51, −0.54[b]
$[ClO_2][Nb_3F_{16}]$	2.40	1.20	−0.21	–	−0.47	−0.53, −0.61[b]
$[ClO_2][Mo_3O_3F_{13}]$	2.02	1.09	−0.17	−0.38	−0.40	−0.46, −0.52[b]
$[ClO_2][Re_3O_6F_{10}]$	2.09	1.19	−0.22	−0.50	−0.36	−0.42, −0.44[b]

[a] Central atom of the anion. [b] μ-Bridging between *M* atoms.

Table 7. Average overlap population between two atoms from Mulliken population analyses of the optimized solid-state structures of $[ClO_2]^+$ salts.

Compound	Average overlap population [*e*]				
	Cl–O	Cl···μ–F	*M* a–O	*M* [a]–F (non-bridging)	*M* [a]–F (bridging)
$[ClO_2][PF_6]$	0.17	0.01	–	0.25	0.22
$[ClO_2][AsF_6]$	0.17	0.01	–	0.29	0.26
$[ClO_2][IrF_6]$	0.17	0.01	–	0.13	0.11
$[ClO_2][SnF_{2/2}F_{4/1}]$	0.18	0.01	–	0.22	0.18, 0.12[b]
$[ClO_2][[TiF_{3/2}F_{3/1}]_2]$	0.18	0.01	–	0.11	0.11, 0.07[b]
$[ClO_2][Nb_3F_{16}]$	0.18	0	–	0.10	0.08, 0.04[b]
$[ClO_2][Mo_3O_3F_{13}]$	0.27	0.01	0.24	0.15	0.14, 0.09[b]
$[ClO_2][Re_3O_6F_{10}]$	0.19	0	0.19	0.13	0.12, 0.07[b]

[a] Central atom of the anion. [b] μ-Bridging between *M* atoms.

to be C_{2v}, resulting in the three possible modes $\nu_3(B_1)$ ($\nu_{as}(ClO_2)$), $\nu_1(A_1)$ ($\nu_s(ClO_2)$) and $\nu_2(A_1)$ ($\delta_{sciss}(ClO_2)$) for the cation.[8] The characteristic and usually most pronounced features in the Raman spectra of the investigated compounds are the bands assigned to the Cl–O stretching modes, $\nu_{as}(ClO_2)$ and $\nu_s(ClO_2)$, which are located at 1283 to 1312 and at 1040 to 1078 cm^{-1}, respectively. The two naturally occurring Cl isotopes ^{35}Cl and ^{37}Cl lead to a splitting of the Cl–O bands, with differences of 13 to 15 cm^{-1} for $\nu_{as}(ClO_2)$ and of 5 to 6 cm^{-1} for $\nu_s(ClO_2)$.[55] The intensities of the bands of $\nu_s(ClO_2)$ is in all cases higher than those of $\nu_{as}(ClO_2)$. The third possible mode is the scissoring of $[ClO_2]^+$, $\delta_{sciss}(ClO_2)$, which can be observed in the range of 513 to 527 cm^{-1}. The experimental and calculated vibrational frequencies are listed in Table 8. Similar vibrational frequencies were reported for $[ClO_2]^+$ in compounds such as $[ClO_2][GeF_5]$, $[ClO_2][MF_6]$ (*M* = Ru, Pt, Au, Sb), $[ClO_2][ClO_4]$, $[ClO_2][Cd(ClO_4)_3]$, $[ClO_2][Au(ClO_4)_4]$ and $[ClO_2][M(ClO_4)_4]$ (*M* = In, Tl).[34,37,40,42,43,115–118] This indicates a minor effect of the anions and bridging atoms (O or F) on the vibrational frequencies of the $[ClO_2]^+$ cation.

The Raman spectra of the $[MF_6]^-$ anions in $[ClO_2][MF_6]$ (*M* = As, Ir) are similar to those of respective Li^+ salts, albeit with more bands due to lower symmetry of the $[MF_6]^-$ anion.[120,121] In the Raman spectrum of $[ClO_2][SnF_{2/1}F_{4/1}]$, an additional band of a $[ClF_2]^+$ cation at 783 cm^{-1} is present, likely due to an impurity of $[ClF_2][SnF_5]$.[122] The Raman spectrum is otherwise similar to the reported one of $[ClO_2]_2[SnF_6]$, which itself has too many bands for

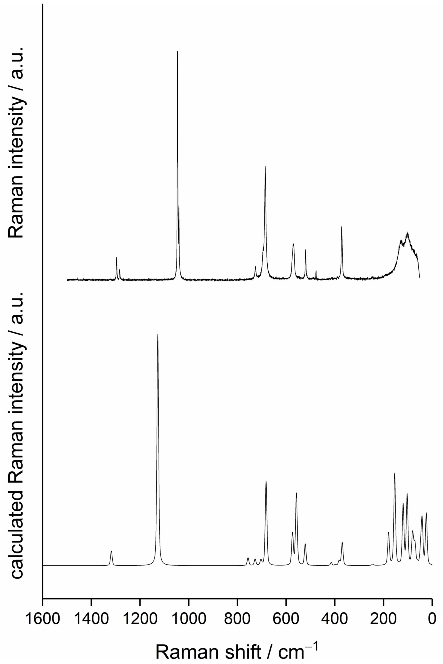

Figure 17. High-resolution (top) and calculated Raman spectrum (bottom) of $[ClO_2][AsF_6]$ with intensities given in arbitrary units.

a $[SnF_6]^{2-}$ salt.[123] They are both similar to those reported for $[NF_4][SnF_5]$ and $[N_2F_3][SnF_5]$.[70,71] The bands assigned to the $[Ti_2F_9]^-$ anion in the Raman spectrum of $[ClO_2][[TiF_{3/2}F_{3/1}]_2]$ are similar to those of $A[Ti_2F_9]$ (A = Cs, NF_4).[92,124] The Raman spectrum of $[ClO_2][Nb_3F_{16}]$ is more complex than that of $Li[NbF_6]$, but similar to that of $[XeF][Nb_2F_{11}]$, with comparable vibrational frequencies for the $v(NbF_6)$ bands.[120,125] The Raman spectrum of $[ClO_2][Mo_3O_3F_{13}]$ is more complex for the anionic part than the reported ones for $A[MoOF_5]$ (A = Cs, Xe_2F_{11}) or $A[Mo_2O_2F_9]$ (A = Li – Cs), which is to be expected.[109,110,126] The Raman spectrum of $[ClO_2][Re_3O_6F_{10}]$ is similar to that of $Cs[Re_3O_6F_{10}]$.[112]

General remarks on the crystal structures of $[ClO_2]^+$ compounds

The $[ClO_2]^+$ cation is bent in the crystal structures of all herein described salts as well as in the previously reported ones. Its structure is in line with the VSEPR model for an AX_2E species.[127] The Cl–O bond lengths of the investigated salts range from 1.384(4) to 1.418(4) Å (Table 2) and are comparable to the Cl–O bond length of 1.418(2) Å determined from the microwave spectrum of gaseous ClO_2F.[128–130] They are much shorter than in solid ClO_2 (1.471(1) and 1.476(1) Å at 123 K).[131] The observed O–Cl–O angles range from 117.37(10) to 119.65(10)°, which is to be expected from the VSEPR model, which predicts an angle below 120° for such a species. In our quantum-chemical calculations, we also obtain angles below 120°. However, in $[ClO_2][Au(ClO_4)_4]$ and $[ClO_2][Sb_2F_{11}]$, the O–Cl–O angles were reported with 132(3) and 121.9(15)°, respectively, likely due to the quality of the structure determinations.[37,44]

The Cl atom of the $[ClO_2]^+$ cation is always surrounded by additional bridging ligands, either F atoms in fluoridometallate or oxidofluoridometallate salts or O atoms in perchlorate-containing compounds.[37–40] The coordination number of the Cl atom in the investigated compounds is usually 2+4, with a distorted octahedral arrangement of the ligands, see Table 9. The only exceptions are $[ClO_2][PF_6]$, in which the coordination number is 2+6 with a distorted square-antiprismatic ligand arrangement, and the previously reported $[ClO_2][GeF_{2/2}F_{4/1}]$ in which Cl atoms with both coordination number 2+4 and 2+6 are present.[42] A range of structural motifs is observed for the $[ClO_2]^+$ salts when the $Cl\cdots\mu{-}F$ interactions are considered. These span from molecular, over column- and ladder-like ones, to layer-like and framework structures and are summarized in Table 9.

Conclusion

The reactions of the main group and transition metal oxides TiO_2, MoO_3, Re_2O_7, SnO, P_2O_5, and As_2O_5 with ClF_3 led to the

Table 8. Comparison of experimental and calculated vibrational frequencies assigned to the $[ClO_2]^+$ cation in compounds with fluoridometallate or oxidofluoridometallate anions.

Compound	$v_{as}(ClO_2)$ [cm^{-1}]	$v_s(ClO_2)$ [cm^{-1}]	$\delta_{sciss}(ClO_2)$ [cm^{-1}]	Reference
$[ClO_2][AsF_6]$	1296, 1283	1046, 1040	519	this work
	1317	1127	521	calculated
	1296	1044, 1039	521	[55]
	1296, 1281	1045	518	[119]
$[ClO_2][IrF_6]$	1290	1061, 1056	518	this work
	1319	1125	521	calculated
	1300, 1286	1057	518	[115]
$[ClO_2][SnF_{2/2}F_{4/1}]$	1303, 1289	1076, 1071	525, 515	this work
	1310, 1306	1136, 1135	532, 530, 520	calculated
$[ClO_2][[TiF_{3/2}F_{3/1}]_2]$	1293, 1280	1049, 1044	517	this work
	1310	1124	516	calculated
$[ClO_2][Nb_3F_{16}]$	1304, 1291	1060, 1054	519	this work
	1320	1135	524	calculated
$[ClO_2][Mo_3O_3F_{13}]$	1309, 1294	1061, 1056	513	this work
	1329	1140	523, 513	calculated
$[ClO_2][Re_3O_6F_{10}]$	1312, 1298	1078, 1072	527	this work
	1316	1135	528	calculated

Table 9. Overview of coordination numbers (C. N.) of the Cl atoms and structure motifs in $[\mathrm{ClO_2}]^+$ fluoridometallates and oxidofluoridometallates.

Compound	C. N. of Cl	Structure motif	Niggli formula
$[\mathrm{ClO_2}][\mathrm{Mo_3O_3F_{13}}]$	2+4	molecular structure (dimeric)	${}_{\infty}^{0}\left[\left[\langle \mathrm{ClF}_{\frac{4}{1+1}}\mathrm{O}_{\frac{2}{1}}\rangle\langle \mathrm{MoF}_{\frac{2}{1+1}}\mathrm{F}_{\frac{1}{2}}\mathrm{F}_{\frac{2}{1}}\mathrm{O}_{\frac{1}{1}}\rangle\langle \mathrm{MoF}_{\frac{2}{2}}\mathrm{F}_{\frac{3}{1}}\mathrm{O}_{\frac{1}{1}}\rangle\langle \mathrm{MoF}_{\frac{1}{1+1}}\mathrm{F}_{\frac{1}{2}}\mathrm{F}_{\frac{3}{1}}\mathrm{O}_{\frac{1}{1}}\rangle\right]_2\right]$
$[\mathrm{ClO_2}][\mathrm{AsF_6}]$	2+4	columnar structure	${}_{\infty}^{1}\left[\langle \mathrm{ClF}_{\frac{2}{2+1}}\mathrm{F}_{\frac{2}{1+1}}\mathrm{O}_{\frac{2}{1}}\rangle\langle \mathrm{AsF}_{\frac{1}{1+2}}\mathrm{F}_{\frac{2}{1+1}}\mathrm{F}_{\frac{3}{1}}\rangle\right]$
$[\mathrm{ClO_2}][[\mathrm{TiF}_{3/2}\mathrm{F}_{3/1}]_2]$	2+4	columnar structure	${}_{\infty}^{1}\left[\langle \mathrm{ClF}_{\frac{4}{1+1}}\mathrm{O}_{\frac{2}{1}}\rangle\langle \mathrm{TiF}_{\frac{2}{1+1}}\mathrm{F}_{\frac{3}{2}}\mathrm{F}_{\frac{1}{1}}\rangle_2\right]$
$[\mathrm{ClO_2}][\mathrm{Re_3O_6F_{10}}]$	2+4	columnar structure	${}_{\infty}^{1}\left[\langle \mathrm{ClF}_{\frac{4}{1+1}}\mathrm{O}_{\frac{2}{1}}\rangle\langle \mathrm{ReF}_{\frac{2}{1+1}}\mathrm{F}_{\frac{1}{2}}\mathrm{F}_{\frac{1}{1}}\mathrm{O}_{\frac{2}{1}}\rangle_2\langle \mathrm{ReF}_{\frac{2}{2}}\mathrm{F}_{\frac{2}{1}}\mathrm{O}_{\frac{2}{1}}\rangle\right]$
$[\mathrm{ClO_2}][\mathrm{Nb_3F_{16}}]$	2+4	ladder-like structure	${}_{\infty}^{1}\left[\langle \mathrm{ClF}_{\frac{4}{1+1}}\mathrm{O}_{\frac{2}{1}}\rangle\langle \mathrm{NbF}_{\frac{2}{1+1}}\mathrm{F}_{\frac{1}{2}}\mathrm{F}_{\frac{3}{1}}\rangle_2\langle \mathrm{NbF}_{\frac{2}{2}}\mathrm{F}_{\frac{4}{1}}\rangle\right]$
$[\mathrm{ClO_2}][M\mathrm{F_6}]$, $M=$ Ru[43], Ir, Sb[34]	2+4	layer structure	${}_{\infty}^{2}\left[\langle \mathrm{ClF}_{\frac{4}{1+1}}\mathrm{O}_{\frac{2}{1}}\rangle\langle \mathrm{IrF}_{\frac{4}{1+1}}\mathrm{F}_{\frac{2}{1}}\rangle\right]$
$[\mathrm{ClO_2}][\mathrm{SnF}_{2/2}\mathrm{F}_{4/1}]$	2+4	layer structure	${}_{\infty}^{2}\left[\langle \mathrm{ClF}_{\frac{2}{2+1}}\mathrm{F}_{\frac{2}{1+1}}\mathrm{O}_{\frac{2}{1}}\rangle\langle \mathrm{SnF}_{\frac{1}{1+2}}\mathrm{F}_{\frac{2}{1+1}}\mathrm{F}_{\frac{2}{2}}\mathrm{F}_{\frac{1}{1}}\rangle\right]$
$[\mathrm{ClO_2}][\mathrm{PF_6}]$	2+6	framework structure	${}_{\infty}^{3}\left[\langle \mathrm{ClF}_{\frac{2}{2+1}}\mathrm{F}_{\frac{4}{1+1}}\mathrm{O}_{\frac{2}{1}}\rangle\langle \mathrm{PF}_{\frac{1}{1+2}}\mathrm{F}_{\frac{4}{1+1}}\mathrm{F}_{\frac{1}{1}}\rangle\right]$
$[\mathrm{ClO_2}][\mathrm{BF_4}]$[41]	2+4	framework structure	${}_{\infty}^{3}\left[\langle \mathrm{ClF}_{\frac{4}{1+1}}\mathrm{O}_{\frac{2}{1}}\rangle\langle \mathrm{BF}_{\frac{4}{1+1}}\rangle\right]$
$[\mathrm{ClO_2}][\mathrm{GeF_5}]$[41,42]	2+4 & 2+6	framework structure	${}_{\infty}^{3}\left[\langle \mathrm{ClF}_{\frac{4}{2+1}}\mathrm{O}_{\frac{2}{1}}\rangle\langle \mathrm{ClF}_{\frac{4}{2+1}}\mathrm{F}_{\frac{2}{1+1}}\mathrm{O}_{\frac{2}{1}}\rangle\langle \mathrm{GeF}_{\frac{2}{1+2}}\mathrm{F}_{\frac{1}{1+1}}\mathrm{F}_{\frac{2}{2}}\mathrm{F}_{\frac{1}{1}}\rangle_2\right]$
$[\mathrm{ClO_2}][\mathrm{Sb_2F_{11}}]$[44]	2+4	framework structure	${}_{\infty}^{3}\left[\langle \mathrm{ClF}_{\frac{4}{1+1}}\mathrm{O}_{\frac{2}{1}}\rangle\langle \mathrm{SbF}_{\frac{2}{1+1}}\mathrm{F}_{\frac{1}{2}}\mathrm{F}_{\frac{3}{1}}\rangle_2\right]$

formation of $[\mathrm{ClO_2}]^+$ compounds with fluoridometallate ($[[\mathrm{Ti}_{3/2}\mathrm{F}_{3/1}]_2]^-$, $[\mathrm{SnF}_{2/2}\mathrm{F}_{4/1}]^-$, $[\mathrm{PF_6}]^-$, $[\mathrm{AsF_6}]^-$) or oxidofluoridometallate ($[\mathrm{Mo_3O_3F_{13}}]^-$, $[\mathrm{Re_3O_6F_{10}}]^-$) anions. The reaction of $\mathrm{ClF_3}$ with oxygen-containing Nb powder, as well as the hydrolysis reaction of $[\mathrm{ClF_2}][\mathrm{IrF_6}]$, led to the formation of $[\mathrm{ClO_2}][\mathrm{Nb_3F_{16}}]$ and $[\mathrm{ClO_2}][\mathrm{IrF_6}]$, respectively. Bent $[\mathrm{ClO_2}]^+$ cations, with Cl–O bond lengths from 1.384(4) to 1.418(4) Å, are present in the crystal structures of these compounds. The Raman bands of the $[\mathrm{ClO_2}]^+$ cations are observed in the range from 1283 to 1312 ($\nu_{as}(\mathrm{ClO_2})$) and from 1040 to 1078 cm^{-1} ($\nu_s(\mathrm{ClO_2})$). The O–Cl–O angles are below 120° in all compounds with 117.37(10) to 119.65(10)°, which is in line with predictions based on the VSEPR model and quantum-chemical calculations. The Cl atom shows furthermore short $\mathrm{Cl}\cdots\mu\text{–F}$ contacts to F atoms from the neighboring anions, resulting in coordination numbers of 2+4 or 2+6 ($[\mathrm{ClO_2}][\mathrm{PF_6}]$) and distorted octahedral or distorted square-antiprismatic arrangements of the ligands. The structure motifs of the $[\mathrm{ClO_2}]^+$ compounds differ a lot and seem to be dictated by the nature of the anion. Quantum-chemical calculations indicate that these $\mathrm{Cl}\cdots\mu\text{–F}$ interactions are weak and ionic. The $[\mathrm{ClO_2}]^+$ cation seems to enable the isolation of rather unusual salts with mono-, bi- and polynuclear anions.

Experimental Section

General: Volatile materials were handled in a Monel metal Schlenk line, which was passivated with undiluted fluorine and/or chlorine trifluoride at various pressures before use. Moisture-sensitive compounds were stored and handled in an Ar-filled glove box (MBraun). Reaction vessels were made out of fluoropolymer (PFA) and closed by stainless-steel valves (SS316 or 316 L, Swagelok). All vessels were passivated with fluorine before use. Preparations were carried out in an atmosphere of dry and purified argon (5.0, Praxair). Chlorine trifluoride was stored over NaF to remove traces of HF. Hydrogen fluoride was stored over $\mathrm{K_2[NiF_6]}$ to remove traces of moisture. **Caution**! *Fluorine, chlorine trifluoride, and dioxychloronium (V) compounds must be handled using appropriate protective gear with ready access to proper emergency treatment procedures in the event of contact. They are potent oxidizing agents that are only stable under the rigorously anhydrous conditions employed in the experimental procedures outlined in this section. They react vigorously to explosively upon hydrolysis or contact with organic materials. The utmost precautions must be taken when disposing of these materials and their derivatives.*

Syntheses – General: A PFA reaction vessel was loaded with the starting material and attached to a stainless-steel valve. The valve was then connected to the Monel metal Schlenk line, the reaction vessel was evacuated and an excess of $\mathrm{ClF_3}$ was condensed onto the solid at 77 K. The reaction vessel was then placed in a stainless-steel Dewar vessel and allowed to warm to room temperature over a period of a few hours. The reaction vessel was then stored at room temperature for the time specified below. All volatiles were then pumped off and the product was isolated in a glove box.

$[\mathrm{ClO_2}][\mathrm{AsF_6}]$, $[\mathrm{ClO_2}][\mathrm{SnF_5}]$, $[\mathrm{ClO_2}][\mathrm{Ti_2F_9}]$, $[\mathrm{ClO_2}][\mathrm{Nb_3F_{16}}]$, $[\mathrm{ClO_2}][\mathrm{Mo_3O_3F_{13}}]$: $[\mathrm{ClO_2}][\mathrm{AsF_6}]$: 14 mg $\mathrm{As_2O_5}$ (0.061 mmol) was reacted with 0.17 g of $\mathrm{ClF_3}$ (1.8 mmol). The reaction vessel was stored at room temperature for two weeks. (25.5 mg isolated) $[\mathrm{ClO_2}][\mathrm{SnF_5}]$: 23.6 mg SnO (0.18 mmol) was reacted with 0.49 g of $\mathrm{ClF_3}$ (5.3 mmol). After that, 0.5 mL of anhydrous HF were condensed on to the reaction mixture at 77 K. The reaction vessel was stored at room temperature for a few hours. Both $[\mathrm{ClO_2}][\mathrm{SnF_5}]$ and a $[\mathrm{ClF_2}]^+$-containing compound were present in the product. $[\mathrm{ClO_2}][\mathrm{Ti_2F_9}]$: 20.0 mg $\mathrm{TiO_2}$ (0.25 mmol) was reacted with 0.15 g of $\mathrm{ClF_3}$ (1.6 mmol). The reaction vessel was stored at room temperature for four days (40.1 mg isolated). $[\mathrm{ClO_2}][\mathrm{Nb_3F_{16}}]$: 10.6 mg Nb powder (0.11 mmol) was reacted with 0.20 g of $\mathrm{ClF_3}$ (2.2 mmol). The reaction vessel was stored at room temperature for one day. Both crystals of $[\mathrm{ClF_2}][\mathrm{NbF_6}]$ and $[\mathrm{ClO_2}][\mathrm{Nb_3F_{16}}]$ were present in the product. $[\mathrm{ClO_2}][\mathrm{Mo_3O_3F_{13}}]$: Method 1: 18.0 mg $\mathrm{MoO_3}$ (0.13 mmol) was reacted with 0.13 g $\mathrm{ClF_3}$ (1.4 mmol). The reaction vessel was stored at room temperature for 19 days (10.7 mg isolated). Method

2: 22.19 mg $MoOF_4$ (0.12 mmol) was reacted with 0.08 g of ClF_3 (0.9 mmol). The reaction vessel was stored at room temperature for eight days (16.0 mg isolated).

Low-temperature syntheses of $[ClO_2][PF_6]$ and $[ClO_2][Re_3O_6F_{13}]$: $[ClO_2][PF_6]$: 10.5 mg P_2O_5 (0.074 mmol) was reacted with 0.12 g of ClF_3 (1.3 mmol). The reaction vessel was then stored at −37 °C and colorless crystals grew at the top of the reaction vessel after a few hours at this temperature. The reaction vessel was then opened to the atmosphere at *circa* −40 °C to isolate some of the crystals for single-crystal X-ray diffraction. They were quickly transferred into cold (*circa* −40 °C) Galden HT270 (perfluoropolyether, Solvay) and handled under a stream of cold nitrogen. Crystals of $[ClO_2][PF_6]$ rapidly deteriorated at room temperature and contact to the atmosphere. $[ClO_2][Re_3O_6F_{13}]$: 19.7 mg Re_2O_7 (0.04 mmol) was reacted with 0.10 g of ClF_3 (1.1 mmol). The reaction vessel was then stored at −37 °C and colorless crystals grew from the yellowish solution after a few hours at this temperature. The reaction vessel was then opened to the atmosphere at < 0 °C to isolate some of the crystals for single-crystal X-ray diffraction. The crystals were handled under cold perfluorinated oil and a stream of cold nitrogen. Crystals of $[ClO_2][Re_3O_6F_{13}]$ rapidly deteriorated at room temperature and contact to the atmosphere.

Hydrolysis of $[ClF_2][IrF_6]$: $[ClO_2][IrF_6]$ was obtained as a hydrolysis product of $[ClF_2][IrF_6]$. 21.9 mg Ir powder (0.11 mmol) was reacted with 0.19 g of ClF_3 (2.1 mmol). The reaction vessel was then stored at −37 °C and yellow crystals grew from the red solution at that temperature after one hour. The reaction vessel was then opened to the atmosphere at < 0 °C to isolate some of the crystals for single-crystal X-ray diffraction. The crystals turned out to be of the compound $[ClF_2][IrF_6]$.[57,59] After that, the reaction vessel was closed again and stored at room temperature for ten days, after which yellow crystals of $[ClO_2][IrF_6]$ grew from the solution.

Single-crystal X-ray diffraction: Crystals of the moisture-sensitive compounds were selected under dried perfluoropolyether (Fomblin YR1800, Solvay, stored over molecular sieve 3 Å) and mounted on a MiTeGen loop. Crystals of $[ClO_2][PF_6]$ and $[ClO_2][Re_3O_6F_{10}]$ were selected in the absence of air under dried, cooled perfluoropolyether (Galden HT270, Solvay, stored over molecular sieves 3 Å) and mounted on a MiTeGen loop. Intensity data of suitable crystals were recorded with a D8 Quest diffractometer (Bruker), an IPDS2, or an IPDS2T diffractometer (STOE). The diffractometers were operated with monochromatized Mo-K_α radiation (0.71073 Å), multi-layered optics (D8 Quest), or a graphite monochromator (IPDS2 and IPDS2T) and equipped with a PHOTON 100 CMOS detector (D8 Quest) or an image plate detector (IPDS2 and IPDS2T). Evaluation, integration, and reduction of the diffraction data was carried out with the APEX3 software suite (D8 Quest) or the X-Area software suite (IPDS2 and IPDS2T).[132,133] The diffraction data were corrected for absorption utilizing the multi-scan method of SADABS or TWINABS within the APEX3 software suite (D8 Quest) or the integration method with the modules X-Shape and X-Red32 of the X-Area software suite (IPDS2 and IPDS2T). The structures were solved with dual-space methods (SHELXT) and refined against F^2 (SHELXL).[134,135] Systematic absence violations were observed for the space groups of the compounds $[ClO_2][PF_6]$ and $[ClO_2][Nb_3F_{16}]$. However, the very weak intensities of the corresponding reflections were very close to the tripled standard uncertainties. The solution and refinement of the structures in crystallographic subgroups resulted in significant correlations between atomic coordinates and non-positive definite displacement parameters for some atoms. The crystal structures were consequently solved and refined in the space groups reported here, which were also indicated by the Addsym feature of the program package PLATON when checking for additional symmetry within the subgroups.[136,137] The crystals of $[ClO_2][IrF_6]$, $[ClO_2][Ti_2F_9]$ and $[ClO_2][Re_3O_6F_{10}]$ used for the diffraction experiment were non-merohedral twins (two twin components in $[ClO_2][IrF_6]$, $[ClO_2][Ti_2F_9]$ and $[ClO_2][Re_3O_6F_{10}]$, respectively). The lattice parameters and twin laws of $[ClO_2][IrF_6]$ and $[ClO_2][Re_3O_6F_{10}]$ were determined with the program CELL_NOW.[138] In the case of $[ClO_2][Ti_2F_9]$, the twin components were determined manually in the X-Area software. In all cases, only the non-overlapping reflections of the major twin component were used for the structure solution. The data were initially refined with all reflections with the HKLF5 format option in SHELXL (overlapping reflections and non-overlapping reflections of all twin components). The data were then processed with the HKLF5Tools program: the non-overlapping reflections of the weaker diffracting twin component were removed, the non-overlapping reflections of the major twin component were merged in point groups 2/*m* ($[ClO_2][IrF_6]$ and $[ClO_2][Ti_2F_9]$) or $\bar{1}$ ($[ClO_2][Re_3O_6F_{10}]$ and the overlapping reflections were merged in point group 1.[139] The final refinements were carried out against the detwinned dataset (created by SHELXL with the LIST 8 option as an FCF file and converted to an HKL file with HKLF5Tools). The locations of highest residual electron densities after the final refinement were the following: $[ClO_2][PF_6]$: 0.38 Å from atom O(2), $[ClO_2][AsF_6]$: 0.76 Å from atom F(1), $[ClO_2][IrF_6]$: 0.63 Å from atom Ir(1), $[ClO_2][SnF_5]$: 0.79 Å from atom Cl(1), $[ClO_2][Ti_2F_9]$: 1.25 Å from atom F(2), $[ClO_2][Nb_3F_{16}]$: 0.57 Å from atom Cl(1), $[ClO_2][Mo_3O_3F_{13}]$: 0.70 Å from atom O(5) and $[ClO_2][Re_3O_6F_{10}]$: 0.70 Å from atom Re(1). Representations of the crystal structures were created with the Diamond software.[140]

Deposition Numbers 2034213 (for $[ClO_2][PF_6]$), 2034214 (for $[ClO_2][AsF_6]$), 2034215 (for $[ClO_2][IrF_6]$), 2034216 (for $[ClO_2][SnF_5]$), 2034217 (for $[ClO_2][Ti_2F_9]$), 2034218 (for $[ClO_2][Nb_3F_{16}]$), 2034219 (for $[ClO_2][Mo_3O_3F_{13}]$), and 2034220 (for $[ClO_2][Re_3O_6F_{10}]$) contain the supplementary crystallographic data for this paper. These data are provided free of charge by the joint Cambridge Crystallographic Data Centre and Fachinformationszentrum Karlsruhe Access Structures service www.ccdc.cam.ac.uk/structures.

Raman spectroscopy: The Raman spectra were measured with a Monovista CRS+ confocal Raman microscope (Spectroscopy & Imaging GmbH) using a 532 nm solid-state laser and either a 300 grooves/mm (low-resolution mode, FWHM: $< 4.62\ cm^{-1}$) or a 1800 grooves/mm (high-resolution mode, FWHM: $< 0.368\ cm^{-1}$) grating. Samples were either transferred into dried glass vessels or immersed in perfluorinated oil (Fomblin YR1800, Solvay, stored over molecular sieve 3 Å) on a microscope slide.

Solid-state quantum-chemical calculations: Periodic quantum-chemical calculations were carried out with the PBE0 hybrid density functional method (DFT-PBE0).[113,114] Triple-zeta-valence + polarization (TZVP) level basis sets were applied for all atoms. Details of the basis sets that were employed are given in the Supporting Information. All calculations were carried out with the CRYSTAL17 program package.[141] The reciprocal space was sampled with the following Monkhorst-Pack-type *k*-point grids: $[ClO_2][PF_6]$: 4×2×2, $[ClO_2][AsF_6]$: 2×2×5, $[ClO_2][IrF_6]$: 3×4×3, $[ClO_2][SnF_5]$: 4×4×4, $[ClO_2][Ti_2F_9]$: 2×2×5, $[ClO_2][Nb_3F_{16}]$: 3×3×3, $[ClO_2][Mo_3O_3F_{13}]$: 3×3×3, $[ClO_2][Re_3O_6F_{10}]$: 3×3×3. For the evaluation of the Coulomb and exchange integrals (TOLINTEG), tight tolerance factors of 8, 8, 8, 8, 16 were used for all calculations. Both the atomic positions and lattice parameters were fully optimized within the constraints imposed by the space group symmetry. Default DFT integration grids and optimization convergence thresholds were applied in all calculations. Mulliken population analyses were carried out for all compounds. A ferromagnetic ground state was employed for $[ClO_2][IrF_6]$ and the resulting magnetic moment was 2.0 μB for the $[IrF_6]^-$ anion (1.4 μB contribution from Ir). The harmonic vibrational frequencies and Raman intensities were obtained through usage of the computational scheme implemented in CRYSTAL17.[142–144] The Raman intensities were calculated for a polycrystalline powder sample (total isotropic intensity in arbitrary units). The Raman spectra were obtained by using a pseudo-Voigt band profile (50:50 Lorentzian:Gaussian) and an FWHM of 8 cm^{-1}. The Raman spectra were simulated taking the experimental setup ($T = 293.15$ K, $\lambda = 532$ nm) into account. The band assignments were carried out by visual inspection of the normal modes with the Jmol program package.[145]

Acknowledgments

We thank the Deutsche Forschungsgemeinschaft (DFG) for generous funding and Dr. Sergei Ivlev (Marburg) for helpful discussions. Open access funding enabled and organized by Projekt DEAL.

Conflict of Interest

The authors declare no conflict of interest.

Keywords: Chlorine · Chlorine trifluoride · Dioxychloronium(V) cations · Fluorine · Structure elucidation

[1] T. D. Cooper, F. N. Dost, C. H. Wang, *J. Inorg. Nucl. Chem.* **1972**, *34*, 3564–3567.
[2] L. Andrews, F. K. Chi, A. Arkell, *J. Am. Chem. Soc.* **1974**, *96*, 1997–2000.
[3] H. S. P. Müller, *Chem. Phys. Lett.* **1999**, *314*, 396–402.
[4] H. S. P. Müller, E. A. Cohen, *J. Chem. Phys.* **2002**, *116*, 2407–2416.
[5] H. Schmitz, H. J. Schumacher, *Z. Anorg. Allg. Chem.* **1942**, *249*, 238–244.
[6] H. Bode, E. Klesper, *Z. Anorg. Allg. Chem.* **1951**, *266*, 275–280.
[7] M. Schmeisser, K. Brändle, in: *Adv. Inorg. Chem. Radiochem.*, Elsevier, **1963**, pp. 41–89.
[8] K. O. Christe, C. J. Schack, in: *Advances in Inorganic Chemistry and Radiochemistry*, Elsevier, **1976**, pp. 319–398.
[9] R. Bougon, J. Isabey, P. Plurien, *C. R. Seances Acad. Sci. Ser. C* **1970**, *271*, 1366–1369.
[10] D. Pilipovich, C. B. Lindahl, C. J. Schack, R. D. Wilson, K. O. Christe, *Inorg. Chem.* **1972**, *11*, 2189–2192.
[11] D. Pilipovich, R. D. Wilson, *Synthesis of Oxychlorine Trifluoride (North American Rockwell Corporation)*, **1972**, US-3,697,394.
[12] A. Engelbrecht, H. Atzwanger, *Monatsh. Chem.* **1952**, *83*, 1087–1089.
[13] K. O. Christe, *Inorg. Nucl. Chem. Lett.* **1972**, *8*, 457–459.
[14] K. O. Christe, R. D. Wilson, *Inorg. Chem.* **1973**, *12*, 1356–1357.
[15] G. H. Rohrback, G. H. Cady, *J. Am. Chem. Soc.* **1947**, *69*, 677–678.
[16] J. E. Sicre, H. J. Schumacher, *Z. Anorg. Allg. Chem.* **1956**, *286*, 232–236.
[17] D. F. Smith, G. M. Begun, W. H. Fletcher, *Spectrochim. Acta* **1964**, *20*, 1763–1770.
[18] K. O. Christe, R. D. Wilson, C. J. Schack, *Inorg. Nucl. Chem. Lett.* **1975**, *11*, 161–163.
[19] A. A. Woolf, *J. Chem. Soc.* **1954**, 4113–4116.
[20] A. J. Arvia, W. H. Basualdo, H. J. Schumacher, *Angew. Chem.* **1955**, *67*, 616–616.
[21] A. J. Arvia, W. H. Basualdo, H. J. Schumacher, *Z. Anorg. Allg. Chem.* **1956**, *286*, 58–80.
[22] H. Bode, E. Klesper, *Angew. Chem.* **1954**, *66*, 605–605.
[23] A. Engelbrecht, *Angew. Chem.* **1954**, *66*, 442–442.
[24] R. Bougon, M. Carles, J. Aubert, *C. R. Seances Acad. Sci. Ser. C* **1967**, *265*, 179–182.
[25] K. O. Christe, *Inorg. Chem.* **1972**, *11*, 1220–1222.
[26] M. Schmeisser, F. L. Ebenhöch, *Angew. Chem.* **1954**, *66*, 230–231.
[27] M. Schmeisser, E. Pammer, *Angew. Chem.* **1955**, *67*, 156–156.
[28] E. Jacob, *Angew. Chem. Int. Ed. Engl.* **1976**, *15*, 158–158.
[29] R. J. Gillespie, P. H. Spekkens, *J. Chem. Soc. Dalton Trans.* **1977**, 1539–1546.
[30] P. H. Spekkens, Oxyfluoro Compounds of Bromine, Dissertation, McMaster University (Canada), **1977**.
[31] R. J. Gillespie, P. H. Spekkens, *Isr. J. Chem.* **1978**, *17*, 11–19.
[32] M. Schmeisser, K. Lang, *Angew. Chem.* **1955**, *67*, 156–156.
[33] J. J. Krasznai, Oxo and Oxyfluoro Complexes of Iodine (V) and (VII), Dissertation, McMaster University (Canada), **1975**.
[34] J. F. Lehmann, S. Riedel, G. J. Schrobilgen, *Inorg. Chem.* **2008**, *47*, 8343–8356.
[35] J.-L. Pascal, J. Potier, C. S. Zhang, *J. Chem. Soc. Dalton Trans.* **1985**, 297.
[36] J.-L. Pascal, F. Favier, *Coord. Chem. Rev.* **1998**, *178–180*, 865–902.
[37] F. Cunin, C. Deudon, F. Favier, B. Mula, J. L. Pascal, *Inorg. Chem.* **2002**, *41*, 4173–4178.
[38] M. Fourati, M. Chaabouni, C. H. E. Belin, J. L. Pascal, J. Potier, *New J. Chem.* **1990**, *14*, 695–700.
[39] K. M. Tobias, M. Jansen, *Angew. Chem. Int. Ed. Engl.* **1986**, *25*, 993–994.
[40] K. M. Tobias, M. Jansen, *Z. Anorg. Allg. Chem.* **1987**, *550*, 16–26.
[41] T. E. Mallouk, G. L. Rosenthal, G. Mueller, R. Brusasco, N. Bartlett, *Inorg. Chem.* **1984**, *23*, 3167–3173.
[42] T. E. Mallouk, B. Desbat, N. Bartlett, *Inorg. Chem.* **1984**, *23*, 3160–3166.
[43] R. Bougon, W. V. Cicha, M. Lance, L. Meublat, M. Nierlich, J. Vigner, *Inorg. Chem.* **1991**, *30*, 102–109.
[44] A. J. Edwards, R. J. C. Sills, *J. Chem. Soc. Dalton Trans.* **1974**, 1726–1729.
[45] K. Seppelt, *Angew. Chem. Int. Ed.* **2019**, *58*, 18928–18930.
[46] K. S. Thanthiriwatte, M. Vasiliu, D. A. Dixon, K. O. Christe, *Inorg. Chem.* **2012**, *51*, 10966–10982.
[47] K. O. Christe, E. C. Curtis, *Inorg. Chem.* **1972**, *11*, 35–39.
[48] R. J. Gillespie, P. Spekkens, *J. Chem. Soc. Dalton Trans.* **1976**, 2391–2396.
[49] L. Helmholz, M. T. Rogers, *J. Am. Chem. Soc.* **1940**, *62*, 1537–1542.
[50] M. Gerken, J. P. Mack, G. J. Schrobilgen, R. J. Suontamo, *J. Fluorine Chem.* **2004**, *125*, 1663–1670.
[51] J.-P. Laval, N. Jennene Boukharrata, *Acta Crystallogr. Sect. C* **2008**, *64*, i47–i49.
[52] Q. Wu, H. Liu, F. Jiang, L. Kang, L. Yang, Z. Lin, Z. Hu, X. Chen, X. Meng, J. Qin, *Chem. Mater.* **2016**, *28*, 1413–1418.
[53] D. K. Huggins, W. B. Fox, *Inorg. Nucl. Chem. Lett.* **1970**, *6*, 337–339.
[54] R. F. Weinland, O. Lauenstein, *Z. Anorg. Chem.* **1899**, *20*, 30–39.
[55] K. O. Christe, C. J. Schack, D. Pilipovich, W. Sawodny, *Inorg. Chem.* **1969**, *8*, 2489–2494.
[56] J. D. Clark, *Ignition! An Informal History of Liquid Rocket Propellants*, Rutgers University Press, New Brunswick, New Jersey, **1972**.
[57] B. Scheibe, R. Haiges, S. I. Ivlev, A. J. Karttunen, U. Müller, K. O. Christe, F. Kraus, *Eur. J. Inorg. Chem.* **2020**, DOI 10.1002/ejic.202000845.
[58] J. Supeł, Ternäre Halogenverbindungen des Rheniums und Technetiums in der Oxidationsstufe +7, Dissertation, Freie Universität Berlin, **2007**.
[59] R. Haiges, in: *Efficient Preparations of Fluorine Compounds* (Ed.: H. W. Roesky), John Wiley & Sons, Inc., Hoboken, NJ, USA, **2012**, pp. 100–107.
[60] S. I. Ivlev, A. J. Karttunen, M. R. Buchner, M. Conrad, F. Kraus, *Angew. Chem. Int. Ed.* **2018**, *57*, 14640–14644.
[61] M. Gerken, M. D. Moran, H. P. A. Mercier, B. E. Pointner, G. J. Schrobilgen, B. Hoge, K. O. Christe, J. A. Boatz, *J. Am. Chem. Soc.* **2009**, *131*, 13474–13489.
[62] C. Röhr, R. Kniep, *Z. Naturforsch. B* **1994**, *49*, 650–654.
[63] W. B. Jensen, in: *Cohesion and Structure* (Eds.: J. Hafner, F. Hulliger, W. B. Jensen, J. A. Majewski, K. Mathis, P. Villars, P. Vogl), North-Holland, **1989**, pp. 105–146.
[64] G. Aminoff, *Z. Kristallogr.* **1923**, *58*, 203–219.
[65] A. Ruiz-Martínez, S. Alvarez, *Chem. Eur. J.* **2009**, *15*, 7470–7480.
[66] W. P. Davey, *Phys. Rev.* **1923**, *21*, 143–161.
[67] H. Fitz, B. G. Müller, O. Graudejus, N. Bartlett, *Z. Anorg. Allg. Chem.* **2002**, *628*, 133–137.
[68] C. Hebecker, H. G. von Schnering, R. Hoppe, *Naturwissenschaften* **1966**, *53*, 154–154.
[69] M. J. Durand, J. L. Galigne, A. Lari-Lavassani, *J. Solid State Chem.* **1976**, *16*, 157–160.
[70] K. O. Christe, C. J. Schack, R. D. Wilson, *Inorg. Chem.* **1977**, *16*, 849–854.
[71] K. O. Christe, C. J. Schack, *Inorg. Chem.* **1978**, *17*, 2749–2754.
[72] W. W. Wilson, A. Vij, V. Vij, E. Bernhardt, K. O. Christe, *Chem. Eur. J.* **2003**, *9*, 2840–2844.
[73] D. Schomburg, R. Krebs, *Inorg. Chem.* **1984**, *23*, 1378–1381.
[74] F. Olbrich, R. J. Lagow, *Z. Anorg. Allg. Chem.* **1995**, *621*, 1929–1932.
[75] C. Bolli, J. Gellhaar, C. Jenne, M. Keßler, H. Scherer, H. Seeger, R. Uzun, *Dalton Trans.* **2014**, *43*, 4326–4334.

[76] B. Alič, M. Tramšek, A. Kokalj, G. Tavčar, *Inorg. Chem.* **2017**, *56*, 10070–10077.
[77] Y. Morgenstern, F. Zischka, A. Kornath, *Chem. Eur. J.* **2018**, *24*, 17311–17317.
[78] Z. Mazej, E. Goreshnik, *Inorg. Chem.* **2020**, *59*, 2092–2103.
[79] K. O. Christe, D. A. Dixon, D. J. Grant, R. Haiges, F. S. Tham, A. Vij, V. Vij, T.-H. Wang, W. W. Wilson, *Inorg. Chem.* **2010**, *49*, 6823–6833.
[80] Z. Mazej, E. Goreshnik, *Eur. J. Inorg. Chem.* **2019**, 1265–1272.
[81] R. L. Davidovich, D. V. Marinin, V. Stavila, K. H. Whitmire, *Coord. Chem. Rev.* **2015**, *299*, 61–82.
[82] I. M. Shlyapnikov, E. A. Goreshnik, Z. Mazej, *Inorg. Chem.* **2018**, *57*, 1976–1987.
[83] G. F. Schäfer, *Z. Kristallogr.* **1986**, *175*, 269–276.
[84] S. Siegel, *Acta Crystallogr.* **1952**, *5*, 683–684.
[85] D. Yu Popov, V. Ya Kavun, A. V. Gerasimenko, V. I. Sergienko, T. F. Antokhina, *Russ. J. Coord. Chem.* **2002**, *28*, 19–24.
[86] R. Fischer, B. G. Müller, *Z. Anorg. Allg. Chem.* **2001**, *627*, 445–452.
[87] J. Ravez, M. Vassiliadis, R. Von der Mühll, P. Hagenmüller, *Rev. Chim. Miner.* **1970**, 967–973.
[88] A. Decken, H. D. B. Jenkins, C. Knapp, G. B. Nikiforov, J. Passmore, J. M. Rautiainen, *Angew. Chem. Int. Ed.* **2005**, *44*, 7958–7961; *Angew. Chem.* **2005**, *117*, 8172–8175.
[89] Z. Mazej, E. Goreshnik, *Eur. J. Inorg. Chem.* **2009**, *2009*, 4503–4506.
[90] I. M. Shlyapnikov, E. A. Goreshnik, Z. Mazej, *Chem. Commun.* **2013**, *49*, 2703–2705.
[91] H. Bialowons, *Z. Anorg. Allg. Chem.* **1995**, *621*, 1223–1226.
[92] Z. Mazej, E. Goreshnik, *Inorg. Chem.* **2009**, *48*, 6918–6923.
[93] I. M. Shlyapnikov, H. P. A. Mercier, E. A. Goreshnik, G. J. Schrobilgen, Z. Mazej, *Inorg. Chem.* **2013**, *52*, 8315–8326.
[94] Z. Mazej, R. Hagiwara, *J. Fluorine Chem.* **2007**, *128*, 423–437.
[95] T. A. Engesser, M. R. Lichtenthaler, M. Schleep, I. Krossing, *Chem. Soc. Rev.* **2016**, *45*, 789–899.
[96] L. R. Morss, N. M. Edelstein, J. Fuger, J J. Katz, Eds., *The Chemistry of the Actinide and Transactinide Elements*, Springer, Dordrecht, **2006**.
[97] B. Scheibe, C. Pietzonka, O. Mustonen, M. Karppinen, A. J. Karttunen, M. Atanasov, F. Neese, M. Conrad, F. Kraus, *Angew. Chem.* **2018**, *130*, 2964–2968; *Angew. Chem. Int. Ed.* **2018**, *57*, 2914–2918.
[98] P. Benkič, H. D. Brooke Jenkins, M. Ponikvar, Z. Mazej, *Eur. J. Inorg. Chem.* **2006**, *2006*, 1084–1092.
[99] E. Goreshnik, Z. Mazej, *J. Fluorine Chem.* **2020**, *236*, 109587.
[100] T. Drews, K. Seppelt, *Angew. Chem. Int. Ed.* **1997**, *36*, 273–274; *Angew. Chem.* **1997**, *109*, 264–266.
[101] A. J. Edwards, G. R. Jones, *J. Chem. Soc. A* **1971**, 2318.
[102] A. J. Edwards, G. R. Jones, *J. Chem. Soc. A* **1970**, 1491–1497.
[103] A. J. Edwards, P. Taylor, *J. Chem. Soc. Dalton Trans.* **1973**, 2150–2153.
[104] F. Marchetti, G. Pampaloni, C. Pinzino, S. Zacchini, *Eur. J. Inorg. Chem.* **2013**, *2013*, 5755–5761.
[105] D. Bizot, *J. Fluorine Chem.* **1978**, *11*, 497–507.
[106] T. Drews, W. Koch, K. Seppelt, *J. Am. Chem. Soc.* **1999**, *121*, 4379–4384.
[107] I. Bernhardi, T. Drews, K. Seppelt, *Angew. Chem. Int. Ed.* **1999**, *38*, 2232–2233; *Angew. Chem.* **1999**, *111*, 2370–2372.
[108] S. M. Rupf, P. Pröhm, M. Malischewski, *Chem. Commun.* **2020**, DOI 10.1039.D0CC04226 A.
[109] M. R. Bortolus, H. P. A. Mercier, G. J. Schrobilgen, *Chem. Eur. J.* **2020**, *26*, 8935–8950.
[110] R. E. Stene, B. Scheibe, A. J. Karttunen, W. Petry, F. Kraus, *Eur. J. Inorg. Chem.* **2019**, *2019*, 3672–3682.
[111] W. L. Bragg, *Philos. Mag.* **1914**, *28*, 355–360.
[112] W. J. Casteel, D. A. Dixon, N. LeBlond, P. E. Lock, H. P. A. Mercier, G. J. Schrobilgen, *Inorg. Chem.* **1999**, *38*, 2340–2358.
[113] J. P. Perdew, K. Burke, M. Ernzerhof, *Phys. Rev. Lett.* **1996**, *77*, 3865–3868.
[114] C. Adamo, V. Barone, *J. Chem. Phys.* **1999**, *110*, 6158–6170.
[115] K. O. Christe, *Inorg. Chem.* **1973**, *12*, 1580–1587.
[116] S. S. Nabiev, *Russ. Chem. Bull.* **1999**, *48*, 711–717.
[117] M. Fourati, M. Chaabouni, J.-L. Pascal, J. Potier, *Can. J. Chem.* **1987**, *65*, 2783–2790.
[118] M. Fourati, M. Chaabouni, H. F. Ayedi, J.-L. Pascal, J. Potier, *Can. J. Chem.* **1985**, *63*, 3499–3504.
[119] H. A. Carter, W. M. Johnson, F. Aubke, *Can. J. Chem.* **1969**, *47*, 4619–4625.
[120] G. Tavčar, B. Žemva, *Inorg. Chem.* **2013**, *52*, 4319–4323.
[121] O. Graudejus, A. P. Wilkinson, L. C. Chacón, N. Bartlett, *Inorg. Chem.* **2000**, *39*, 2794–2800.
[122] A. I. Popov, A. V. Scharabarin, V. F. Sukhoverkhov, N. A. Tchumaevsky, *Z. Anorg. Allg. Chem.* **1989**, *576*, 242–254.
[123] H. A. Carter, A. M. Qureshi, J. R. Sams, F. Aubke, *Can. J. Chem.* **1970**, *48*, 2853–2859.
[124] K. O. Christe, C. J. Schack, *Inorg. Chem.* **1977**, *16*, 353–359.
[125] B. Landa, Laser Raman Spectroscopic Investigations of Some Fluoroxenon Compounds, Dissertation, McMaster University (Canada), **1974**.
[126] A. Beuter, W. Sawodny, *Z. Anorg. Allg. Chem.* **1976**, *427*, 37–44.
[127] R. J. Gillespie, R. S. Nyholm, *Q. Rev. Chem. Soc.* **1957**, *11*, 339–380.
[128] C. R. Parent, M. C. L. Gerry, *J. Mol. Spectrosc.* **1974**, *49*, 343–364.
[129] A. G. Robiette, C. R. Parent, M. C. L. Gerry, *J. Mol. Spectrosc.* **1981**, *86*, 455–464.
[130] H. S. P. Müller, *J. Mol. Struct.* **2000**, *517–518*, 335–350.
[131] A. Rehr, M. Jansen, *Inorg. Chem.* **1992**, *31*, 4740–4742.
[132] *APEX3*, Bruker AXS Inc., Madison, Wisconsin, USA, **2018**.
[133] *X-Area*, STOE & Cie GmbH, Darmstadt, Germany, **2018**.
[134] G. M. Sheldrick, *Acta Crystallogr. Sect. A* **2015**, *71*, 3–8.
[135] G. M. Sheldrick, *Acta Crystallogr. Sect. C* **2015**, *71*, 3–8.
[136] A. L. Spek, *PLATON – A Multipurpose Crystallographic Tool*, Utrecht University, Utrecht, The Netherlands, **2019**.
[137] A. L. Spek, *Acta Crystallogr. Sect. D* **2009**, *65*, 148–155.
[138] G. M. Sheldrick, *CELL_NOW*, Göttingen (Germany), **2008**.
[139] S. I. Ivlev, M. Conrad, F. Kraus, *Z. Kristallogr.* **2019**, *234*, 415–418.
[140] K. Brandenburg, H. Putz, *Diamond – Crystal and Molecular Structure Visualization*, Crystal Impact GbR, Bonn, **2019**.
[141] R. Dovesi, A. Erba, R. Orlando, C. M. Zicovich-Wilson, B. Civalleri, L. Maschio, M. Rérat, S. Casassa, J. Baima, S. Salustro, B. Kirtman, *Wiley Interdiscip. Rev.: Comput. Mol. Sci.* **2018**, e1360.
[142] C. M. Zicovich-Wilson, F. Pascale, C. Roetti, V. R. Saunders, R. Orlando, R. Dovesi, *J. Comput. Chem.* **2004**, *25*, 1873–1881.
[143] F. Pascale, C. M. Zicovich-Wilson, F. López Gejo, B. Civalleri, R. Orlando, R. Dovesi, *J. Comput. Chem.* **2004**, *25*, 888–897.
[144] L. Maschio, B. Kirtman, M. Rérat, R. Orlando, R. Dovesi, *J. Chem. Phys.* **2013**, *139*, 164101.
[145] *Jmol: An Open-Source Java Viewer for Chemical Structures in 3D. Http://Www.Jmol.Org/*, Jmol Team, **2019**.

Manuscript received: September 29, 2020
Revised manuscript received: November 6, 2020
Accepted manuscript online: November 7, 2020